Supplemental Material For:

Topologically associating domains and their role in the evolution of genome structure and function in *Drosophila*

Yi Liao[1,†], Xinwen Zhang[1], Mahul Chakraborty[1] and J.J. Emerson[1,2,†]

[1]Department of Ecology and Evolutionary Biology, University of California, Irvine, CA, USA.

[2]Center for Complex Biological Systems, University of California, Irvine, CA, USA.

[†]Email: liaoy12@uci.edu and jje@uci.edu

Supplemental Methods

QV estimation and BUSCO validation for the *D. pseudoobscura* assembly

We applied the method of Koren et al. (Koren et al. 2018) to the polished, pre-scaffolded assemblies to estimate base level error rates from the concordance between Illumina reads and the assembly of the same strain (i.e. QV).

Freebayes version v0.9.21 was run with the command:

freebayes -C 2 -0 -O -q 20 -z 0.10 -E 0 -X -u -p 2 -F 0.75 -b Dpseu.sorted.bam -v dpse.bayes.vcf -f Dpseudo_PacBioV2_genomic.fna

We calculated BUSCOs in our assembly with BUSCO V3 against the Diptera and Arthropoda database (Waterhouse et al. 2017).

Genome Annotation

Simple Tandem repeats, centromeric and telomeric repeats identification Tandem repeats were identified using Tandem repeat finder (Benson 1999) with parameters “2 7 7 80 10 50 2000 -f -d -m”. The top 5 most abundant consensus sequences of tandemly repeated units were used as queries for further searching against the genome assembly to check their chromosomal distributions and the abundant frequency in the genome using RepeatMasker (http://www.repeatmasker.org/). Based on this information, we identified two centromere-specific tandem repeats in *D. pseudoobscura*, with the motif size of 170 bp and 21 bp, respectively. The 170-bp tandem repeat is only detected on the X and dot chromosome and is absent from its closely related species, *D. miranda*, suggesting the rapid turnover of centromere-specific repeats between species and even across chromosomes within species in *Drosophila*.

Transposable elements annotation TE annotation was mainly performed using the EDTA pipeline. We also ran the following additional utilities to identify additional transposable elements in *D. pseudoobscura* genome. First, we applied RepeatModeler version 1.0.11 (Smit et al. 2015) for *de novo* repeat sequences identification with the default parameters. The resulting transposable elements library was filtered to exclude elements that overlapping with gene features based on Blastn. In total, RepeatModeler generated 924 candidate TE families,

covering 1,149,638 bp. Next, we employed LTR_retriever pipeline (Ou and Jiang 2018) to specifically annotate long terminal repeat (LTR) retrotransposons in the *D. pseudoobscura* and *D. miranda* genomes. This pipeline outline is as follows: LTR retrotransposons were first identified using LTRharvest (Ellinghaus, Kurtz, and Willhoeft 2008) with parameters: -similar 90 -vic 10 -seed 20 -seqids yes -minlenltr 100 -maxlenltr 7000 -mintsd 4 -maxtsd 6 -motif TGCA -motifmis 1; then LTR_FINDER (Xu and Wang 2007) was run with parameters: -D 15000 -d 1000 -L 7000 -l 100 -p 20 -C -M 0. The output from the utilities above was combined and processed using LTR_retriever to obtain intact LTR-RT elements and construct a non-redundant LTRs library. Using LTR_retriever, we identified a total of 470 and 1,927 (of them, 1,406 located on the new Y chromosome) intact LTR-RT elements for *D. pseudoobscura* and *D. miranda*, respectively. We also employed MITE_Hunter (Han and Wessler 2010) and GRF https://github.com/bioinfolabmu/GenericRepeatFinder to identify Miniature Inverted repeat Transposable Elements (MITE). These two programs generated a total of 149 families of MITEs.

By searching the Repbase *Drosophila* TE library, the custom LTR retrotransposon library from LTR_retriever and the custom MITE sequences from MITE_Hunter and GRF, we were able to assign the TE type for 797/924 of RepeatModeler non-redundant repeat families, including 454 LTR retrotransposable elements and 343 DNA-type elements. The final custom TE library we generated for *D. pseudoobscura* integrates results from Repbase, LTR_retriver, the MITE annotation, and the RepeatModeler output.

Gene annotation In this study, we performed *de novo* gene annotation for *D. miranda* (Mahajan et al. 2018) and *D. pseudoobscura* using Maker (version 2.31.8)(Campbell et al. 2014), following https://gist.github.com/darencard/bb1001ac1532dd4225b030cf0cd61ce2. For *D. miranda*, we assembled a transcriptome with data from using two publicly available RNA-seq datasets (Nozawa et al. 2016; Mahajan et al. 2018), composed of 12 and 21 samples, respectively. These samples cover a wide range of tissues and developmental stages for both male and female. RNA-seq reads from each sample were individually aligned to the genome assembly using HiSat2 (Kim et al. 2015) and assembled by StringTie (Pertea et al. 2015) with the default parameters. The resulting gtf files for each sample were then merged into a single file using the Stringtie --merge function. To prepare transcript evidence for

MAKER, the merged gtf files were converted to gff files using gffread. The transcriptome sequences were extracted accordingly using ReSeqTools (He et al. 2013) based on the gff file and reference genome. For protein evidence, the amino acid sequences from *D. melanogaster* (Flybase r6.26) and *D. pseudoobscura* (r3.04) were used.

For *D. pseudoobscura*, we used transcripts obtained from Flybase (r3.04) and a recent re-annotation project (Yang et al. 2018), each containing 23,456 and 39,527 transcripts, respectively. In addition, we generated the transcriptome using RNA-seq data from a previous study (Nozawa et al. 2016). Moreover, in order to achieve more accurate gene models and identify high-confidential alternative splice transcripts, a total of 15,372 and 22,237 Full-length Isoforms obtained from ISO-seq sequencing in male and female, respectively, were also integrated to guide gene annotation in the MAKER pipeline. Protein evidence used for *D. pseudoobscura* gene annotation includes translated sequences from *D. melanogaster* (Flybase r6.26) and protein sequences annotated for *D. miranda* in this study. The MAKER pipeline was run three times for each species.

Single-molecule RNA sequencing (Iso-seq) experiment and data analysis

Total RNA was extracted from the adult full bodies for males and females, respectively, using RNeasy Plus Mini Kit (Cat No./ID: 74134). cDNA synthesis and library preparation was performed at UC Irvine GHTF. One SMRT cell for each sex sample was sequenced using PacBio Sequel I. ISO-seq data was processed following the *IsoSeq* v3 pipeline which is available at https://github.com/PacificBiosciences/IsoSeq.

HiC Experiments

The Arima-HiC experiment was performed as follows: First, adult female flies were crosslinked as whole animals using 2% formaldehyde. After crosslinking, flies were pulverized on dry ice with mortar and pestle and then subject to the Arima-HiC protocol described in the Arima-HiC kit. Briefly, pulverized crosslinked fly tissue was digested using a cocktail or restriction enzymes recognizing the GATC and GANTC motifs. Next, digested ends were labeled, proximally ligated, and then proximally-ligated DNA was purified. After the Arima-HiC protocol, Illumina-compatible sequencing libraries were prepared by first shearing purified Arima-HiC proximally-ligated DNA and then size-selecting ~400bp DNA fragments using SPRI beads. The

size-selected fragments containing ligation junctions were enriched using Enrichment Beads provided in the Arima-HiC kit, and converted into Illumina-compatible sequencing libraries using the KAPA Hyper Prep kit (P/N: KK8504) reagents. After unique dual index adapter ligation, DNA was PCR amplified and purified using SPRI beads. The purified DNA underwent standard QC (qPCR and Bioanalyzer) and sequenced on the HiSeq X following the manufacturer's protocols.

Gene Ontology analysis and identification of constitutive genes

Gene Ontology analysis was performed using the online tool available at the GO project website http://geneontology.org/. To identify constitutive genes in *D. melanogaster*, we used the expression data obtained from 8 tissues for both sex in two strains (w1118 and oreR) for *D. melanogaster* (Yang et al. 2018). We defined constitutive genes as those genes have expression level larger than 5 (gene-level DESeq2 normalized read counts) in all tissues (8), repilcations (4), sex (2), and strains (2). In total, 5854 genes meet this criteria.

Assembly-based structural variants detection pipeline

Our assembly-based structural variant detection pipeline includes four key steps: (1) Soft masked query genomes are aligned against the reference genome using LASTZ (Version 1.04). (2) The resulting Axt alignment files from step 1 are used to build long genome alignment chains (i.e. connect alignments if they are close enough) using axtChain. The chain files were sorted and merged into a single file using chainMergeSort if necessary. Next, a filtering procedure was applied to remove the low-quality chains using chainPreNet and the keeping chains were then used to get alignment nets by running chainNet. Finally, synteny information was added using netSyntenic. (3) SV calling for each pairwise genome comparison was performed using our custom Perl scripts based on the final syntenic format file from step 2. The SV output includes insertion, deletion, tandem duplication, inversion and complex SVs. (4) Population-scale genotyping of SVs was performed using custom Perl scripts. The custom Perl scripts for this pipeline are available at https://github.com/yiliao1022/LASTZ_SV_pipeline and https://github.com/yiliao1022/TADEvoDrosophila/tree/master/5_SVs_Calling.

Evaluation of the relative abundance of SVs at TAD boundaries

We measured the relative abundance of structural variants at TAD boundaries following a previously described method (Fudenberg and Pollard 2019). The method compares the observed number of SVs and the amount of sequences these SVs affected within the genomic regions where annotated as TAD boundaries with a uniform genome-wide expectation, which imposes the simplifying assumption that the SV mutation rate is fairly similar across the genome. In total, 8.62 Mb (4 kbp plus 2,156) was annotated as TAD boundary regions in *D. melanogaster*. For analysis in *D. pseudoobscura*, we used the 5-kbp HiCExplorer boundaries**.** The observed/expected count and base coverage of SVs were calculated according to the formula: $(\sum_{i \in k} N_i)/(N_{total} \sum_{i \in k} \frac{S_i}{S_{total}})$, where i indexes genomic regions annotated as TAD boundaries, S_{total} is the genome size, and N_{total} is the total number and base coverage of each type of SV genomewide. SVs that fall into the heterochromatin and centromeric regions were excluded from the analysis, as these regions may be more prone to variants artifacts.

Supplemental Tables

Supplemental Table S1: Sequencing data for *D. pseudoobscura* genome assembling.

PacBio			Illumina paired-end			Hi-C		
Reads	Mean Length	Depth	Pairs	Length	Depth	Pairs	Length	Depth
3,170,985	14,493 bp	~280	154,932,139	150bp	~283	397,020,516	150bp	~726

Depth is calculated based on the genome size of 164 MB.

Supplemental Table S2: Assembly statistics for the *D. pseudoobscura* genome.

Features	Scaffold	Contig
Number	70	72
Total Bases	163,274,969	163,282,969
N10	68,158,638	35,530,770
N30	68,158,638	32,422,566
N50	32,422,566	30,706,867
N70	30,706,867	23,510,042
N80	30,706,867	22,902,128
N90	23,510,042	9,717,740
Min	1,117	1,117
Max	68,158,638	35,530,770

	Length	Contig Number	NCBI accession
Chr2	32,422,566	1	CM020868.1
Chr3	23,510,042	1	CM020869.1
Chr4	30,706,867	1	CM020870.1
Chr5	1,881,070	1	CM020871.1
ChrX	68,158,638	3	CM020872.1
Mitochondrion	16,118	1	CM020873.2
Unplace	6,587,668	64	-

Supplemental Table S3: Quality evaluation of the current *D. pseudoobscura* genome assembly.

Quality Value (QV) = -10log$_{10}$(Probability of error)		52	
		Diptera_odb9	**Arthropoda_odb9**
BUSCO score	Complete BUSCOs (C)	2731 (97.6%)	1061 (99.5%)
	Complete and single-copy BUSCOs (S)	2700 (96.5%)	1047 (98.2%)
	Fragmented BUSCOs (F)	31 (1.1%)	14 (1.3%)
	Missing BUSCOs (M)	42 (1.5%)	1 (0.1%)
	Total BUSCO groups searched	26 (0.9%)	4 (0.4%)
		2799	1066

Supplemental Table S4: Sequence composition of the 64 unplaced contigs.

TE occupancy	Centromeric repeats: Simple repeats: Small RNA: Retroelements: DNA transposon: Unclassified:	3,639,793 bp 71,045 bp 263,447 bp 2,211,064 bp 26,375 bp 453,477 bp	54 % 1 % 4 % 33 % 0.4 % 6.8 %
Contigs contains centromere-specific tandem repeats	170bp WVEN01000009.1 WVEN01000011.1 WVEN01000012.1 WVEN01000013.1 WVEN01000014.1 WVEN01000015.1 WVEN01000016.1 WVEN01000018.1 WVEN01000020.1 WVEN01000022.1 WVEN01000028.1 WVEN01000041.1 WVEN01000042.1 WVEN01000044.1 WVEN01000045.1 WVEN01000046.1 WVEN01000047.1 WVEN01000048.1 WVEN01000049.1 WVEN01000050.1 WVEN01000054.1 WVEN01000055.1 WVEN01000056.1 WVEN01000057.1 WVEN01000058.1 WVEN01000065.1 WVEN01000066.1	21bp WVEN01000008.1 WVEN01000019.1 WVEN01000021.1 WVEN01000023.1 WVEN01000029.1 WVEN01000060.1 WVEN01000061.1	Both WVEN01000026.1 WVEN01000043.1 WVEN01000059.1

Contig Names refer to NCBI GenBank assembly accession GCF_009870275.2

Supplemental Table S5: Comparison of assembly continuity for existing *D. pseudoobscura* genome assemblies.

Continuity		Flybase r3.04	Dpse_4.0 (English et al. 2012)	(Bracewell et al. 2019)	(Miller et al. 2018)	This study
	(Strain)	(MV2-25)	(MV2-25)	-	(MV2-25)	(MV-25-SWS-2005)
N10	(bp)	568,313	31,355,180	20,319,488	7,334,445	35,530,770
N30	(bp)	304,883	30,679,157	9,603,404	4,302,182	32,422,566
N50	(bp)	156,571	26,005,469	5,757,666	2,983,193	30,706,867
N70	(bp)	74,128	22,861,174	1,827,199	1,033,991	23,510,042

Supplemental Table S6: Gene and TE annotation for the *D. pseudoobscura* genome.

Gene Models		**BUSCO score (Diptera_odb9)**	
Chromosome	**Number**		
Chr2	3,287	C:95.0%[S:62.8%,D:32.2%],F:2.5%,M:2.5%,n:2799	
Chr3	2,545		
Chr4	2,564	2658	Complete BUSCOs (C)
Chr5	74	1757	Complete and single-copy BUSCOs (S)
X	4,292	901	Complete and duplicated BUSCOs (D)
Mitochondrion	13	70	Fragmented BUSCOs (F)
Unplaced	638	71	Missing BUSCOs (M)
Total	13,413	2799	Total BUSCO groups searched

Repetitive sequences		
Centromeric repeats:	4,851,739 bp	2.97 %
Simple repeats:	7,656,035 bp	4.69 %
Retro-elements:	22,773,268 bp	13.95 %
DNA transposons:	1,985,898 bp	1.22 %
Unclassified	6,660,145 bp	4.08%

Supplemental Table S7: RNA sequencing data used for gene annotation in the MAKER pipeline.

Data	NCBI accession	Tissue	Reference
Published RNA-seq	From DRR055234 to DRR055275	**Tissues including:** abdomens; Male accessory glands; abdomens without gonads; imaginal discs; heads; 3rd instar larvae; 3rd instar larvae without imaginal discs; Female ovaries; pupae; thoraxes; Male testes; adult;	(Nozawa et al. 2016)
Published transcripts			
39,527 transcripts	GSE99574	Details see GSE99574	(Yang et al. 2018)
23,456 transcripts	NA	NA	FlyBase r3.04
ISO-seq			
15,372 transcripts	PRJNA596268	Male adult full body	This study
22,237 transcripts	PRJNA596268	Female adult full body	This study

Supplemental Table S8: Hi-C data preprocessing.

	HiCExplorer		3dDNA
Pairs considered	397,020,516	**Sequenced Read Pairs**	397,020,516
Pairs mappable, unique and high quality	304,513,515 (76.70%)	Alignable (Normal+Chimeric Paired)	337,748,332 (85.1%)
Pairs used (Hi-C Contacts)	194,589,768 (**49.01%**)	Paired used (Hi-C Contacts)	204,080,597 (**51.4%**)
Inter chromosomal	9,275,009 (2.3%)	Inter chromosomal	7,746,309 (2.0%)
Intra chromosomal		Intra chromosomal	
Short range (<20 kbp)	74,173,026 (18.7%)	Short range (<20 kbp)	99,160,171 (25.0%)
Long range	111,141,733 (28.0%)	Long range	97,172,702 (24.5%)

Supplemental Table S9: Synteny blocks between *D. melanogaster* (BDGP Release 6) and *D. pseudoobscura* (this study).

Supplemental Table S9A: *D. melanogaster to D. pseudoobscura*

	Intrachromosomal		Interchromosomal		
	Number of Syntenic blocks	Syntenic coverage	Number of Syntenic blocks	Syntenic coverage	Base Coverage
2L	163	19,489,042	1	81,462	16,062,093
2R	157	17,105,335	1	16,682	14,630,878
3L	152	18,854,583	5	69,854	16,580,574
3R	210	24,793,351	0	0	21,277,942
4	29	895,323	0	0	406,947
X	217	15,483,353	50	3,243,056	12,146,805
Total	928	96,620,987	57	3,411,054	81,105,239

Supplemental Table S9B: *D. pseudoobscura to D. melanogaster*

	Intrachromosomal		Interchromosomal		
	Number of Syntenic blocks	Syntenic coverage	Number of Syntenic blocks	Syntenic coverage	Base Coverage
Chr2	210	26,818,840	6	129,583	22,275,738
Chr3	157	17,119,684	0	0	15,090,175
Chr4	163	23,133,097	1	4,662	17,083,083
Chr5	29	846379	0	0	456,074
XR	152	20,096,070	50	4,026,659	19,857,440
XL	217	17,063,934	0	0	10,747,531
Total	**928**	**105,078,004**	**57**	**4,160,904**	**85,510,041**

Supplemental Table S10: TADs identified in different cell lines/tissues and tools.

Species/ cell lines		Armatus		HiCExporer		Arrowhead	Ref.
Dmel	Num.	Cov.	Num.	Cov.	Num.	Cov.	
Kc167	914	79 Mb	933	131 Mb	698	76 Mb	(Chathoth and Zabet 2019)
BG3	979	76 Mb	956	131 Mb	609	63 Mb	
S2	1,005	72 Mb	1,107	132 Mb	624	63 Mb	(Wang et al. 2018)
Dpse							
Full body	858	95.8 Mb	1013	146 Mb	795	87.4 Mb	This study

Only considered TAD size > 30 kbp for Armatus in *Dps*e and > 20 kbp in *Dmel*;
Num., Number of TADs;
Cov., genome coverage;

Supplemental Table S11: Permutation tests (n=10,000) for determining if the observed conservation rates were significant than expected.

Features	Samples	Observation	Expectation[d]	95% confidence interval	*P*-values
Body[a]	*Dmel* (Kc167)	291/640	68	55 - 86	1×10^{-4}
	Dmel (BG3)	308/668	71	58 - 89	1×10^{-4}
	Dmel (S2)	325/792	74	60 - 92	1×10^{-4}
	Dpse (WB)	419/678	101	86 - 116	1×10^{-4}
Body[b]	*Dmel* (Kc167)	465	210	190 - 229	1×10^{-4}
	Dmel (BG3)	496	221	201 - 241	1×10^{-4}
	Dmel (S2)	601	280	257 - 302	1×10^{-4}
	Dpse (WB)	534	252	232 - 274	1×10^{-4}
		[C/L]	[C/L]	[C/L]	
Boundary[c]	*Dmel* (Kc167)	331/683	87/774	70 - 105 / 752 - 796	2.2×10^{-16}
	Dmel (BG3)	339/722	90/801	73 - 108 / 779 - 822	2.2×10^{-16}
	Dmel (S2)	351/807	103/924	86 - 123 / 899 - 947	2.2×10^{-16}
	Dpse (WB)	494/768	135/757	114 -157 / 730 - 783	2.2×10^{-16}

[a] hypothesis first;

[b] alternative hypothesis;

[c]5 kbp boundary for *Dmel* and 10 kbp boundary for *Dpse*;

[d]Expectation was determined by the mean of the 10,000 simulated samples;

(*Dmel*) *D. melanogaster*;

(*Dpse*) *D. pseudoobscura*;

(WB) whole body;

(C/L) Conserved/lifted over TADs.

Supplemental Table S12: Summary of TAD annotation (HiCExplorer), lift and conservation between *D. melanogaster* (BDGP Release 6) and *D. pseudoobscura* (this study).

TAD Features	Species (sample)	Total	Liftover success	Conserved[a]	Genome Cov. [C/L/T] (Mb)	*P* values
Body	*Dmel* (Kc167)	933	640 (68.6%)	182 (19.5%)	27.9/88.2/131.4	1×10^{-4}
	Dmel (BG3)	964	668 (69.3%)	179 (18.6%)	28.5/90.0/131.3	1×10^{-4}
	Dmel (S2)	1,107	792 (71.5%)	173 (15.6%)	24.4/91.5/132.4	1×10^{-4}
	Dpse (WB)	1,013	678 (66.9%)	284 (28.0%)	43.6/90.5/145.6	1×10^{-4}

[a]Conservation was determined by **90%** reciprocal overlap cutoff;
(*Dmel*) *D. melanogaster*;
(*Dpse*) *D. pseudoobscura*;
(Genome Cov.) Genome coverage, which was calculated for total annotated TADs (T), successfully lifted TADs (L) and conserved TADs based on the genome of the original species;
P values were calculated using permutation tests (n=10,000).

Supplemental Table S13: Published ChIP-seq or ChIP-chip data sources used in this study.

Species	Cell /tissue	Insulator proteins	Accession	Reference
D. melanogaster	S2	BEAF32	GSE20760	(Schwartz et al. 2012)
D. melanogaster	S2	CP190	GSE20766	Schwartz et al. 2012
D. melanogaster	S2	CTCF	GSE32818	Riddle et al. 2011)
D. melanogaster	S2	Chromator	GSE20765	modENCODE
D. melanogaster	S2	Su(Hw)	GSE32813	(Riddle et al. 2011)
D. melanogaster	S2	Trl	GSE32822	Riddle et al. 2011
D. melanogaster	Kc167	BEAF32	GSM762845	(Wood et al. 2011)
D. melanogaster	Kc167	CP190	GSM762836	Wood et al. 2011
D. melanogaster	Kc167	CTCF	GSM1535983	Wood et al. 2011
D. melanogaster	Kc167	Chromator	GSM1318357/GSE20763	Wood et al. 2011
D. melanogaster	Kc167	Su(Hw)	GSM762839/GSE51964	Wood et al. 2011
D. melanogaster	Kc167	Trl	modEncode_3245	modENCODE
D. melanogaster	BG3	BEAF32	GSE20811	Schwartz et al. 2012
D. melanogaster	BG3	CP190	GSE20814	Schwartz et al. 2012
D. melanogaster	BG3	CTCF	GSE20767	Schwartz et al. 2012
D. melanogaster	BG3	Chromator	GSE20761	modENCODE
D. melanogaster	BG3	Su(Hw)	GSE20833	Schwartz et al. 2012
D. melanogaster	BG3	Trl	GSE23466	modENCODE
D. pseudoobscura	Embryos	BEAF-32	-	(Yang et al. 2012)
D. pseudoobscura	WP	CTCF	-	(Ni et al. 2012)

Supplemental Table S14: Evolutionary conservation of different TAD boundary classes between *D. melanogaster* and *D. pseudoobscura* (Supplemental to Figure 3).

Supplemental Table S14A: *Genomic background expectation obtained from simulating 10,000 samples of randomized 10-kbp TAD boundaries.*

Total number	Successfully lifted over	Expected conservation rate
1673	1324	198/1324 = 15%

Supplemental Table S14B: *TAD boundaries that overlapped with distinct insulator binding sites.*

Cell lines /Methods	Insulator	Conserved overlapped	Total	Percent	Conserved without overlapped	Total	Percent	*P*-values
Kc167								
HiCExplorer	BEAF	278	456	0.61	93	196	0.47	0.001875
	CTCF	163	273	0.60	208	379	0.55	0.2512
	Chro	325	532	0.61	46	120	0.38	8.783e-06
	SuHw	227	392	0.58	144	260	0.55	0.578
	GAF	124	210	0.59	247	442	0.56	0.4978
	CP190	304	519	0.59	67	133	0.50	0.1084
Juicer	BEAF	252	401	0.63	367	662	0.55	0.02097
	CTCF	167	258	0.65	452	805	0.56	0.01832
	Chro	335	520	0.64	284	534	0.53	0.00027
	SuHw	272	452	0.60	347	611	0.57	0.2968
	GAF	119	221	0.54	500	842	0.59	0.1589
	CP190	329	525	0.63	290	538	0.54	0.004593
Armatus	BEAF	534	747	0.71	315	635	0.50	2.2e-16
	CTCF	320	438	0.73	529	944	0.56	2.109e-09
	Chro	654	918	0.71	195	464	0.42	2.2e-16
	SuHw	481	727	0.66	368	655	0.56	0.000177
	GAF	270	404	0.67	579	978	0.59	0.009613
	CP190	622	901	0.69	227	481	0.47	3.072e-15
BG3								
HiCExplorer	BEAF	60	98	0.61	332	623	0.54	0.1749
	CTCF	78	154	0.51	314	567	0.55	0.3402
	Chro	349	602	0.58	43	119	0.36	1.957e-0
	SuHw	101	194	0.53	291	527	0.55	0.5027
	GAF	178	320	0.56	214	401	0.53	0.5964
	CP190	254	428	0.59	138	293	0.47	0.001542
Juicer	BEAF	36	68	0.53	514	933	0.55	0.8276
	CTCF	102	169	0.60	448	832	0.54	0.1427
	Chro	320	546	0.59	230	455	0.51	0.01285
	SuHw	158	290	0.54	392	711	0.55	0.9063
	GAF	170	313	0.54	380	688	0.55	0.8395

	CP190	228	389	0.59	322	612	0.53	0.07285
Armatus	BEAF	102	149	0.68	772	1,352	0.57	0.009881
	CTCF	162	280	0.58	712	1,221	0.58	0.9424
	Chro	704	1061	0.66	170	440	0.39	2.2e-16
	SuHw	240	475	0.51	634	1,026	0.62	4.902e-05
	GAF	366	609	0.60	508	892	0.57	0.2457
	CP190	497	778	0.64	377	723	0.52	5.239e-06
S2								
HiCExplorer	BEAF	328	580	0.57	77	215	0.36	3.128e-07
	CTCF	49	103	0.48	356	692	0.51	0.5301
	Chro	367	648	0.57	38	147	0.26	2.941e-11
	SuHw	68	143	0.48	337	652	0.52	0.4218
	GAF	190	361	0.53	215	434	0.50	0.4254
	CP190	336	620	0.54	69	175	0.39	0.000766
Juicer	BEAF	262	459	0.57	234	525	0.46	0.000118
	CTCF	51	101	0.50	445	883	0.50	1
	Chro	325	566	0.57	171	418	0.41	4.277e-07
	SuHw	90	183	0.49	406	801	0.51	0.7751
	GAF	137	279	0.49	359	705	0.51	0.6575
	CP190	294	516	0.57	202	468	0.43	2.003e-05
Armatus	BEAF	594	904	0.66	215	563	0.38	2.2e-16
	CTCF	100	175	0.57	709	1,292	0.55	0.6278
	Chro	662	1021	0.65	147	446	0.33	2.2e-16
	SuHw	159	345	0.46	650	1,122	0.58	0.000141
	GAF	301	516	0.58	508	951	0.53	0.07964
	CP190	629	1036	0.611	180	431	0.42	4.393e-11

Supplemental Table S14C: Stronger versus weaker TAD boundaries.

	Total Num. of stronger borders	Num. of conserved strong borders	Percent	Total Num. of of weaker borders	Num. of conserved weaker borders	Percent	*P*-values
Dmel to *Dpse*							
Kc167	292	196	0.67	393	186	0.47	3.757e-07
BG3	347	220	0.63	396	181	0.46	1.995e-06
S2	430	261	0.61	394	153	0.39	5.617e-10
Dpse to *Dmel*							
Kc167	367	235	0.64	326	130	0.40	3.373e-10
BG3	367	225	0.61	326	132	0.40	6.782e-08
S2	367	243	0.66	326	142	0.44	3.344e-09

Supplemental Table S14D: *TAD boundaries that are shared across cell lines versus cell-specific boundaries.*

Methods	Total Num.of shared borders	Conserved shared borders	Percent	Total Num. of cell-specific borders	Conserved cell-specific borders	Percent	*P*-values
Armatus	1757	1180	0.67	943	405	0.43	2.2e-16
Hicexplorer	672	392	0.58	483	165	0.34	8.309e-16
Juicer	1229	753	0.61	795	299	0.38	2.2e-16

Supplemental Table S14E: *TAD boundary classes with different flanking chromatin modifications.*

Chromatin combinations	Total Num. of boundary	Num. of conserved boundary	Percent	*P*-values
Active_Active	659	262	0.40	0.002325[a]
Active_PcG	342	152	0.44	8.119e-05[b]
Active_Inactive	665	287	0.43	2.336e-05[c]
Inactive_Inactive	233	73	0.31	-
Inactive_PcG	166	62	0.37	-
PcG_PcG	141	33	0.23	-
Inactive_total	540	168	0.31	-
Total	2245	881	0.39	-
Randomization test	2245	476	0.21	-

Inactive_total = sum (Inactive_Inactive + Inactive_PcG + PcG_PcG);
[a]*P*-value was calculated for Active_Active versus Inactive_total;
[b]*P*-value was calculated for Active_PcG versus Inactive_total;
[c]*P*-value was calculated for Active_Inactive versus Inactive_total;
Note: *P*-values from Supplemental Table S14 A,B,C,D are determined by Chi-squared test.

Supplemental Table S15: Both strong and weak TAD boundaries are more frequently shared with boundaries that were identified across cell types, whereas weak TAD boundaries are more frequently overlapped with cell-specific boundaries than strong ones.

	Cell-specific (752)	**Across-cell-types** (921)	***P*-values**
Kc167			
Strong (413)	59	354	
Weak (576)	151	392	2.802×10^{-7}
BG3			
Strong (441)	53	388	
Weak (568)	160	384	1.37×10^{-11}
S2			
Strong (584)	135	449	
Weak (569)	221	318	8.332×10^{-11}

P-values are determined by Fisher exact test.

Supplementary Table S16: 129 long (>50 kbp) coding genes coincided with full TADs in *D. melanogaster*.

Dmel geneID	Gene name	Chr	Start	End	*Dpse* ortholog	*Dpse* geneID	Chr	Start	End
FBgn0000479									
FBgn0003256									
FBgn0004198									
FBgn0052580									
FBgn0085638									
FBgn0266199									
FBgn0267033									
FBgn0267336									
FBgn0284236									
FBgn0003963	ush	2L	476220	540560	FBgn0075472	LOC4817316	NC_046681.1	18886568	18962765
FBgn0041111	lilli	2L	2885929	2954406	FBgn0081331	LOC4816631	NC_046681.1	5205103	5303786
FBgn0015600	toc	2L	3068345	3144786	FBgn0246841	LOC6903567	NC_046681.1	10160973	10211507
FBgn0051774	fred	2L	3902928	3991713	FBgn0076481	LOC4816819	NC_046681.1	19828341	19951473
FBgn0000547	ed	2L	4031377	4115749	FBgn0071799	LOC4817240	NC_046681.1	19639096	19758672
FBgn0003716	tkv	2L	5219000	5271384	FBgn0072755	LOC4817227	NC_046681.1	24852925	24919964
FBgn0085450	Snoo	2L	7891187	7984196	FBgn0080091	LOC4817376	NC_046681.1	23141739	23255965
FBgn0011259	Sema1a	2L	8542147	8672041	FBgn0074948	LOC4816208	NC_046681.1	14892768	15012903
FBgn0041092	tai	2L	9166778	9250211	FBgn0072098	LOC4816259	NC_046681.1	15388231	15481384
FBgn0032151	nAChRalpha6	2L	9793317	9886250	FBgn0077986	LOC4817310	NC_046681.1	18110288	18208112
FBgn0051721	Trim9	2L	10544883	10628054	FBgn0079380	LOC4816752	NC_046681.1	6696732	6769563
FBgn0259176	bun	2L	12455540	12546611	FBgn0247162	LOC6902896	NC_046681.1	20992639	21111231
FBgn0263354	CG42784	2L	13415431	13500427	FBgn0246640	LOC6903438	NC_046681.1	12668130	12693940
FBgn0259984	kuz	2L	13550139	13639411	FBgn0080133	LOC4818148	NC_046681.1	12755253	12871144
FBgn0028509	CenG1A	2L	13835564	13898712	FBgn0076510	LOC4816443	NC_046681.1	3648729	3710205
FBgn0261563	wb	2L	14263027	14328262	FBgn0073665	LOC4816591	NC_046681.1	4185195	4261530
FBgn0003016	osp	2L	14599196	14689340	FBgn0077483	LOC4818069	NC_046681.1	11488589	11613073
FBgn0028863	CG4587	2L	15644183	15718272	FBgn0078284	LOC4816419	NC_046681.1	5020033	5066453
FBgn0259735	mtgo	2L	16545016	16663218	FBgn0247420	LOC6903125	NC_046681.1	26136170	26267233
FBgn0261804	CG42750	2L	18159811	18275770	FBgn0080155	LOC4817320	NC_046681.1	22488603	22544365
FBgn0058006	CG40006	2L	22622417	22756349	FBgn0265242	LOC6902757	NC_046681.1	2952011	2974803
FBgn0263780	CG17684	2R	1866080	2262115	FBgn0246910	LOC6903318	NC_046681.1	17564336	17570127
FBgn0260995	dpr21	2R	3066499	3191011	FBgn0272884	LOC26533897	NC_046681.1	17771326	17783592
FBgn0040849	Ir41a	2R	4917519	5021955	FBgn0245983	LOC6898024	NC_046680.1	3767355	3769951
FBgn0053554	Nipped-A	2R	5177965	5251022	FBgn0245413	LOC26533571	NC_046680.1	1398559	1548443
FBgn0000546	EcR	2R	6087873	6169087	FBgn0243551	LOC6899016	NC_046680.1	21585943	21671815
FBgn0086655	jing	2R	6502006	6621792	FBgn0263814	LOC6899052	NC_046680.1	21772166	21902528
FBgn0003090	pk	2R	7150703	7223378	FBgn0070804	LOC4803477	NC_046680.1	4966792	5020419

FBgn0033438	Mmp2	2R	9611139	9683858	FBgn0245614	LOC6898791	NC_046680.1	17885883	17960741
FBgn0261698	SLO2	2R	10322195	10416996	FBgn0071943	LOC4804232	NC_046680.1	10892329	10984572
FBgn0263102	psq	2R	10557888	10617280	FBgn0264580	LOC6898873	NC_046680.1	19855085	19902889
FBgn0053144	CG33144	2R	10740054	10798709	FBgn0077331	LOC4805321	NC_046680.1	19716315	19755708
FBgn0000633	CG17716	2R	13623044	13749367	FBgn0074649	LOC4805164	NC_046680.1	18229569	18358516
FBgn0265974	ttv	2R	14526267	14587917	FBgn0070143	LOC4803961	NC_046680.1	8788651	8853115
FBgn0264089	sli	2R	15869495	15922118	FBgn0263810	LOC4805561	NC_046680.1	21507934	21562752
FBgn0285917	sbb	2R	18278198	18357296	FBgn0245672	LOC6898650	NC_046680.1	15255540	15329626
FBgn0003435	sm	2R	19517864	19631508	FBgn0264769	LOC4804945	NC_046680.1	16339804	16441091
FBgn0010415	Sdc	2R	21392402	21481176	FBgn0070413	LOC4805278	NC_046680.1	19298122	19391643
FBgn0266129	lov	2R	25085780	25139627	FBgn0265027	LOC4804618	NC_046680.1	13839121	13849504
FBgn0035094	CG9380	2R	25183628	25255318	FBgn0081730	LOC4804620	NC_046680.1	13921798	13927626
FBgn0001316	klar	3L	434083	540614	FBgn0074321	LOC117184056	NC_046679.1	17232815	17233267
FBgn0267487	Ptp61F	3L	1342493	1475257	FBgn0081581	LOC4812118	NC_046683.1	64577786	64585987
FBgn0266696	Svil	3L	2377655	2499226	FBgn0076834	LOC4812804	NC_046683.1	55075034	55211476
FBgn0263392	Tet	3L	2786207	2879158	FBgn0249681	LOC6900088	NC_046683.1	65557238	65659194
FBgn0262593	Shab	3L	2895017	2959579	FBgn0249911	LOC6900092	NC_046683.1	65471782	65527489
FBgn0262870	axo	3L	4629604	4687317	FBgn0074906	LOC4812589	NC_046683.1	59089541	59153919
FBgn0035574	RhoGEF64C	3L	4692783	4796253	FBgn0249899	LOC6900063	NC_046683.1	59158565	59284682
FBgn0085447	sif	3L	5657913	5749599	FBgn0078858	LOC4813607	NC_046683.1	50614964	50710357
FBgn0020251	sfl	3L	6495680	6550104	FBgn0080991	LOC4814130	NC_046683.1	66608453	66672946
FBgn0261788	Ank2	3L	7655389	7718395	FBgn0245004	LOC6900405	NC_046683.1	44181432	44250541
FBgn0016694	Pdp1	3L	7811458	7867369	FBgn0249858	LOC4812101	NC_046683.1	57972383	58017080
FBgn0011817	nmo	3L	7979046	8054147	FBgn0249744	LOC6899982	NC_046683.1	57785259	57853064
FBgn0085385	bma	3L	9908120	9967298	FBgn0244878	LOC6900645	NC_046683.1	50839836	50897100
FBgn0041096	rols	3L	12008225	12064859	FBgn0076690	LOC4812739	NC_046683.1	60074493	60128691
FBgn0260941	app	3L	12206238	12266841	FBgn0079009	LOC4813857	NC_046683.1	45062249	45128414
FBgn0264001	bru3	3L	13521907	13803400	FBgn0262083	LOC6900229	NC_046683.1	62237844	62554451
FBgn0087007	bbg	3L	14412828	14536276	FBgn0081889	LOC4813512	NC_046683.1	49738548	49857900
FBgn0259175	ome	3L	14672839	14747868	FBgn0076726	LOC4813899	NC_046683.1	43509178	43577286
FBgn0261090	Sytbeta	3L	15014695	15064977	FBgn0075740	LOC4813079	NC_046683.1	43181391	43225404
FBgn0260943	Rbp6	3L	17058774	17238212	FBgn0244751	LOC6900901	NC_046683.1	55683847	55875214
FBgn0016797	fz2	3L	19140975	19235373	FBgn0081984	LOC4812483	NC_046683.1	61926741	61929000
FBgn0262737	mub	3L	21844788	21932702	FBgn0080346	LOC4813190	NC_046683.1	47711136	47763777
FBgn0004449	Ten-m	3L	22293044	22407863	FBgn0246553	LOC6903600	NC_046683.1	56595766	56737063
FBgn0266347	nAChRalpha4	3L	23206669	23287448	FBgn0071670	LOC4811728	NC_046679.1	18978998	19036653
FBgn0287185	nvd	3L	24324866	24401655	FBgn0272278	LOC26533291	NC_046679.1	19042190	19046707
FBgn0267429	lovit	3L	25236940	25670980	FBgn0263149	LOC6897476	NC_046679.1	19205188	19215147
FBgn0287183	l(3)80Fg	3L	25798441	26014112	FBgn0270973	LOC26531986	NC_046679.1	18926361	18949519

FBgn0267430	Pzl	3R	2554162	3263582	FBgn0246990	LOC6899548	NC_046679.1	26030363	26054844
FBgn0263346	smash	3R	4659579	4712193	FBgn0263296	LOC6897751	NC_046679.1	25020967	25036713
FBgn0013576	mtd	3R	5270116	5350443	FBgn0248772	LOC6897619	NC_046679.1	22529751	22600472
FBgn0083949	side-III	3R	5862865	5959555	FBgn0248644	LOC6897387	NC_046679.1	16350190	16436589
FBgn0083963	Nlg3	3R	7570281	7639434	FBgn0247584	LOC6897868	NC_046679.1	27586270	27676356
FBgn0266801	CG45263	3R	8364328	8477617	FBgn0076231	LOC4802637	NC_046679.1	24064667	24177705
FBgn0261929	5-HT2B	3R	8578205	8629996	FBgn0080752	LOC4802031	NC_046679.1	17586939	17634157
FBgn0262614	pyd	3R	8827068	8931896	FBgn0263173	LOC4802625	NC_046679.1	23926197	24041582
FBgn0003165	pum	3R	9066343	9237682	FBgn0263302	LOC6899331	NC_046679.1	25150068	25361033
FBgn0001235	hth	3R	10507561	10639568	FBgn0074358	LOC4801015	NC_046679.1	7419554	7526298
FBgn0037963	Cad87A	3R	11893512	11949129	FBgn0248851	LOC6897810	NC_046679.1	26173815	26206576
FBgn0264493	rdx	3R	13967061	14032057	FBgn0082107	LOC4801646	NC_046679.1	13899676	13970122
FBgn0285955	cv-c	3R	14391683	14481713	FBgn0076192	LOC4801949	NC_046679.1	16632194	16724764
FBgn0263929	jvl	3R	14741582	14795868	FBgn0077532	LOC4801060	NC_046679.1	7994919	8070854
FBgn0266756	btsz	3R	14804092	14875488	FBgn0248064	LOC6897024	NC_046679.1	8084537	8136265
FBgn0259244	CG42342	3R	16502770	16571363	FBgn0262050	LOC6896920	NC_046679.1	5650062	5712218
FBgn0263995	cpo	3R	17919832	18018892	FBgn0076133	LOC4803162	NC_046679.1	29609529	29684944
FBgn0004652	fru	3R	18414273	18545586	FBgn0262676	LOC4801442	NC_046679.1	12163419	12258033
FBgn0263974	qin	3R	18591027	18650137	FBgn0072931	LOC4801434	NC_046679.1	11990290	12061241
FBgn0003118	pnt	3R	23290231	23346167	FBgn0262662	LOC6897112	NC_046679.1	9813046	9884417
FBgn0051145	CG31145	3R	23605751	23669659	FBgn0248188	LOC6896811	NC_046679.1	3196002	3278400
FBgn0004509	Fur1	3R	25347431	25473058	FBgn0263364	LOC6897901	NC_046679.1	28168848	28337718
FBgn0011666	msi	3R	25516118	25608423	FBgn0248760	LOC6897597	NC_046679.1	21943710	22050910
FBgn0039431	plum	3R	26470078	26535217	FBgn0079629	LOC4801081	NC_046679.1	8225629	8289170
FBgn0004842	RYa-R	3R	26996980	27057935	FBgn0262494	LOC13036374	NC_046679.1	8807721	8868130
FBgn0004369	Ptp99A	3R	29377646	29487131	FBgn0263238	LOC4800475	NC_046679.1	2268638	2383280
FBgn0266411	sima	3R	30058311	30121798	FBgn0080705	LOC4800293	NC_046679.1	729199	793552
FBgn0010113	hdc	3R	30277932	30372382	FBgn0262041	LOC6896726	NC_046679.1	361603	444621
FBgn0261988	Gprk2	3R	31405245	31457873	FBgn0074786	LOC4800727	NC_046679.1	4750576	4790127
FBgn0284435	tyn	X	142208	200663	FBgn0244270	LOC6901851	NC_046683.1	22322415	22367122
FBgn0052816	CG32816	X	316576	470726	FBgn0077175	LOC4815282	NC_046683.1	14038292	14061888
FBgn0264449	CG43867	X	808217	927975	FBgn0243670	LOC6901139	NC_046683.1	39399697	39543032
FBgn0025390	Mur2B	X	1523554	1668788	FBgn0244397	LOC6902079	NC_046683.1	40512867	40519529
FBgn0283741	prage	X	1773719	1853667	FBgn0073294	LOC4815930	NC_046683.1	4167796	4202646
FBgn0052791	DIP-alpha	X	3507245	3571649	FBgn0244620	LOC6901640	NC_046683.1	9241195	9268292
FBgn0266429	AstA-R1	X	3574536	3666724	FBgn0075512	LOC4814982	NC_046683.1	9393504	9418311
FBgn0283657	Tlk	X	3720007	3789770	FBgn0247156	LOC6901632	NC_046683.1	9488755	9586869
FBgn0000635	Fas2	X	4132887	4206093	FBgn0077610	LOC4814416	NC_046683.1	39288156	39368197
FBgn0029881	pigs	X	6600062	6653015	FBgn0077823	LOC4815731	NC_046683.1	22102264	22159609

FBgn0261873	sdt	X	8178549	8240474	FBgn0077114	LOC4814721	NC_046683.1	14168679	14235710
FBgn0261260	mgl	X	9358496	9500129	FBgn0071481	LOC4816002	NC_046683.1	2983510	3010620
FBgn0052698	CARPB	X	9783223	9855449	FBgn0243764	LOC6901062	NC_046683.1	1115681	1163504
FBgn0259170	alpha-Man-Ia	X	10266792	10325958	FBgn0077085	LOC4811663	NC_046683.1	9116064	9182650
FBgn0085443	spri	X	10490069	10585422	FBgn0247809	LOC6901478	NC_046683.1	12339033	12451658
FBgn0267001	Ten-a	X	12043698	12335214	FBgn0077061	LOC4815803	NC_046683.1	42182177	42397715
FBgn0259171	Pde9	X	12785563	12897327	FBgn0077055	LOC4814257	NC_046683.1	38534763	38676799
FBgn0264078	Flo2	X	14839376	14933946	FBgn0244429	LOC6902140	NC_046683.1	4923878	5025517
FBgn0000535	eag	X	14955477	15009989	FBgn0244430	LOC6902148	NC_046683.1	4848589	4889314
FBgn0285944	para	X	16455027	16533096	FBgn0082095	LOC4814623	NC_046683.1	15180603	15252555
FBgn0266354	CG45002	X	16969069	17066732	FBgn0248789	LOC6901200	NC_046683.1	17251805	17361961
FBgn0003380	Sh	X	17924307	18063247	FBgn0247929	LOC6901448	NC_046683.1	12898779	13029681
FBgn0265598	Bx	X	18515428	18572809	FBgn0247290	LOC6902855	NC_046681.1	20210853	20212694
FBgn0264090	CG43759	X	18930335	19028629	FBgn0076989	LOC4814891	NC_046683.1	7320033	7439102

Note: Coordinates in *D. melanogaster* are based on reference genome version BDGP Release 6; Coordinates and gene IDs in *D. pseudoobscura* are based on the GenBand assembly accession GCA_009870125.2.

Supplementary Table S17: 73 long (>50 kbp) coding genes coincided with full TADs in *D. pseudoobscura*.

Dpse	Chr	Start	End	Flybase geneID	*Dmel* ortholog	Gene name	Chr	Start	End
LOC6896811	NC_046679.1	3196002	3278400	FBgn0248188	FBgn0051145	CG31145	3R	23605751	23669659
LOC4800781	NC_046679.1	5386959	5438514	FBgn0077383	FBgn0053208	Mical	3R	10001554	10042895
LOC6896916	NC_046679.1	5461116	5578166						
LOC6896920	NC_046679.1	5650062	5712218	FBgn0262050	FBgn0259244	CG42342	3R	16502770	16571363
LOC4800948	NC_046679.1	6763020	6834216	FBgn0248101	FBgn0037546	mAChR-B	3R	8059284	8087049
LOC4801003	NC_046679.1	7189395	7246437	FBgn0079305	FBgn0004876	cdi	3R	19044882	19094270
LOC6897007	NC_046679.1	7732765	7790727	FBgn0248077	FBgn0262617	Nuak1	3R	10264306	10308467
LOC4801081	NC_046679.1	8225629	8289170	FBgn0079629	FBgn0039431	plum	3R	26470078	26535217
LOC6897112	NC_046679.1	9813046	9884417	FBgn0262662	FBgn0003118	pnt	3R	23290231	23346167
LOC4801646	NC_046679.1	13899676	13970122	FBgn0082107	FBgn0264493	rdx	3R	13967061	14032057
LOC4801764	NC_046679.1	14784567	14835704	FBgn0247893	FBgn0053100	eIF4EHP	3R	24063077	24108960
LOC4801843	NC_046679.1	15359555	15533548	FBgn0075943	FBgn0011224	heph	3R	31846987	32015520
LOC6897387	NC_046679.1	16350190	16436589	FBgn0248644	FBgn0083949	side-III	3R	5862865	5959555
LOC4801949	NC_046679.1	16632194	16724764	FBgn0076192	FBgn0285955	cv-c	3R	14391683	14481713
LOC4802074	NC_046679.1	17817447	17894364	FBgn0243536	FBgn0003944	Ubx	3R	16656623	16734426
LOC4802304	NC_046679.1	21082351	21136455	FBgn0261650	FBgn0085386	CG34357	3R	4491943	4558067
LOC4802625	NC_046679.1	23926197	24041582	FBgn0263173	FBgn0262614	pyd	3R	8827068	8931896
LOC6899331	NC_046679.1	25150068	25361033	FBgn0263302	FBgn0003165	pum	3R	9066343	9237682
LOC26534216	NC_046679.1	26295215	26353745	FBgn0247625	FBgn0264357	SNF4Agamma	3R	21140739	21214269
LOC6897868	NC_046679.1	27586270	27676356	FBgn0247584	FBgn0083963	Nlg3	3R	7570281	7639434
LOC6897901	NC_046679.1	28168848	28337718	FBgn0263364	FBgn0004509	Fur1	3R	25347431	25473058
LOC4803056	NC_046679.1	28349791	28404616	FBgn0263363	FBgn0262582	cic	3R	20252770	20303942
LOC6899355	NC_046679.1	28625913	28734691	FBgn0249366	FBgn0038755	Hs6st	3R	19929277	20008512
LOC4803264	NC_046679.1	30602446	30780262	FBgn0263373	FBgn0260003	Dys	3R	19461085	19597288
LOC4803646	NC_046680.1	6343075	6410100	FBgn0075887	FBgn0040752	Prosap	2R	14060456	14140902
LOC4804232	NC_046680.1	10892329	10984572	FBgn0071943	FBgn0261698	SLO2	2R	10322195	10416996
LOC6898462	NC_046680.1	11786375	11861598	FBgn0245753	FBgn0013733	shot	2R	13864237	13942110
LOC4804516	NC_046680.1	12998411	13067112	FBgn0072699	FBgn0033405	CG13954	2R	9309296	9389467
LOC6898564	NC_046680.1	13825579	13905008	FBgn0246243	FBgn0054038	CG34038	2R	25167659	25169855
LOC6898642	NC_046680.1	15005173	15069436	FBgn0245675	FBgn0002643	mam	2R	13991203	14060356
LOC6898647	NC_046680.1	15163374	15249936	FBgn0245674	FBgn0053958	CG33958	2R	18184382	18192851
LOC4804945	NC_046680.1	16339804	16441091	FBgn0264769	FBgn0003435	sm	2R	19517864	19631508
LOC6898791	NC_046680.1	17885883	17960741	FBgn0245614	FBgn0033438	Mmp2	2R	9611139	9683858
LOC4805263	NC_046680.1	19176666	19251051	FBgn0075833	FBgn0041239	Gr58a	2R	21979860	21981099
LOC4805278	NC_046680.1	19298122	19391643	FBgn0070413	FBgn0010415	Sdc	2R	21392402	21481176
LOC6898874	NC_046680.1	19914625	19976308	FBgn0264579	FBgn0283521	lola	2R	10481894	10543291
LOC4805422	NC_046680.1	20762914	20815098	FBgn0072148	FBgn0033667	reb	2R	11904323	11912779
LOC4805561	NC_046680.1	21507934	21562752	FBgn0263810	FBgn0264089	sli	2R	15869495	15922118
LOC6899052	NC_046680.1	21772166	21902528	FBgn0263814	FBgn0086655	jing	2R	6502006	6621792
LOC4805739	NC_046680.1	23319395	23407484	FBgn0080886	FBgn0023441	fus	2R	15657318	15676669
LOC4816443	NC_046681.1	3648729	3710205	FBgn0076510	FBgn0028509	CenG1A	2L	13835564	13898712
LOC4816591	NC_046681.1	4185195	4261530	FBgn0073665	FBgn0261563	wb	2L	14263027	14328262
LOC6903561	NC_046681.1	10275293	10366559	FBgn0246567	FBgn0016977	spen	2L	159032	203397
LOC4818069	NC_046681.1	11488589	11613073	FBgn0077483	FBgn0003016	osp	2L	14599196	14689340

LOC4817896	NC_046681.1	12699950	12749976	FBgn0081619	FBgn0023407	B4	2L	13500624	13549328
LOC4818148	NC_046681.1	12755253	12871144	FBgn0080133	FBgn0259984	kuz	2L	13550139	13639411
LOC26533542	NC_046681.1	14293071	14349942						
LOC4816208	NC_046681.1	14892768	15012903	FBgn0074948	FBgn0011259	Sema1a	2L	8542147	8672041
LOC4816259	NC_046681.1	15388231	15481384	FBgn0072098	FBgn0041092	tai	2L	9166778	9250211
LOC6902405	NC_046681.1	15579131	15732776	FBgn0249459	FBgn0000464	Lar	2L	19586623	19732069
LOC4817865	NC_046681.1	16393823	16474646	FBgn0076373	FBgn0266521	stai	2L	6100377	6124653
LOC4817310	NC_046681.1	18110288	18208112	FBgn0077986	FBgn0032151	nAChRalpha6	2L	9793317	9886250
LOC4816903	NC_046681.1	18235141	18286585	FBgn0075064	FBgn0028704	Nckx30C	2L	9711512	9746495
LOC4817316	NC_046681.1	18886568	18962765	FBgn0075472	FBgn0003963	ush	2L	476220	540560
LOC4817453	NC_046681.1	19120954	19177483	FBgn0078274	FBgn0004611	Plc21C	2L	305935	355566
LOC6902868	NC_046681.1	20531988	20656719	FBgn0272756					
LOC6902896	NC_046681.1	20992639	21111231	FBgn0247162	FBgn0259176	bun	2L	12455540	12546611
LOC4817376	NC_046681.1	23141739	23255965	FBgn0080091	FBgn0085450	Snoo	2L	7891187	7984196
LOC6903125	NC_046681.1	26136170	26267233	FBgn0247420	FBgn0259735	mtgo	2L	16545016	16663218
LOC4817542	NC_046681.1	26739952	26812700	FBgn0073723	FBgn0053516	dpr3	2L	2058790	2109878
LOC6903295	NC_046681.1	29801894	29908866	FBgn0249104	FBgn0034106	CG9068	2R	16283435	16287450
LOC4811795	NC_046682.1	784082	839864	FBgn0074773	FBgn0085432	pan	4	69326	114270
LOC4815782	NC_046683.1	3474993	3530448	FBgn0074848	FBgn0004370	Ptp10D	X	11622015	11677338
LOC6901756	NC_046683.1	6654611	6736259	FBgn0249613	FBgn0029946	CG15034	X	7346259	7347506
LOC6901632	NC_046683.1	9488755	9586869	FBgn0247156	FBgn0283657	Tlk	X	3720007	3789770
LOC6901448	NC_046683.1	12898779	13029681	FBgn0247929	FBgn0003380	Sh	X	17924307	18063247
LOC26532449	NC_046683.1	25938122	26018820						
LOC6901093	NC_046683.1	38284146	38417666	FBgn0243698	FBgn0265597	rad	X	12988615	13079070
LOC6901139	NC_046683.1	39399697	39543032	FBgn0243670	FBgn0264449	CG43867	X	808217	927975
LOC6902018	NC_046683.1	41866256	41951315	FBgn0244155	FBgn0264542	hwt	X	12516634	12568452
LOC4813557	NC_046683.1	45301101	45446946	FBgn0076932	FBgn0262509	nrm	3L	22998372	23040300
LOC6900681	NC_046683.1	51484002	51610780	FBgn0245227	FBgn0052062	Rbfox1	3L	10481412	10594012
LOC4812408	NC_046683.1	61629954	61730871	FBgn0076771	FBgn0052206	CG32206	3L	19340321	19412912

Note: Coordinates in *D. melanogaster* are based on reference genome version BDGP Release 6; Coordinates and gene IDs in *D. pseudoobscura* are based on the GenBank assembly accession GCA_009870125.2.

Supplemental Table S18: Genome synteny breakpoints (within synteny blocks larger than 10 kbp) identified in the other 16 *Drosophila* genome assemblies relative to *D. melanogaster* and *D. pseudoobscura*, respectively.

	Divergence Time (Mys)	Top fills	Nonsyn fills	Syntenic fills	Inv fills	Total syntenic breaks	Total inversion breaks
***D. melanogaster* versus**							
D. simulans	3.53	101	9	3	13	121	13
D. mauritiana	3.53	144	12	3	14	167	14
D. sechellia	3.53	123	8	4	10	143	10
D. erecta	7.25	90	6	4	22	108	22
D. yakuba	7.25	112	10	5	16	135	16
D. eugracilis	14.27	178	55	4	19	245	19
D. biarmipes	15.24	85	158	18	38	269	38
D. triauraria	Unknown	627	115	9	36	759	36
D. ananassae	34.37	189	237	59	106	493	106
D. bipectinata	34.37	540	219	7	22	774	22
D. pseudoobscura	49	169	9	246	314	432	314
D. persimilis	49	385	281	35	101	709	101
D. miranada	49	187	30	223	308	448	308
D. willistoni	62.1	1001	163	8	63	1180	63
D. mojavensis	72.63	879	123	16	58	1026	58
D. virilis	72.63	729	184	41	91	962	91
***D. pseudoobscura* versus**							
D. simulans	49	232	324	94	144	678	172
D. mauritiana	49	265	286	101	164	681	193
D. sechellia	49	197	323	112	159	661	188
D. melanogaster	49	181	4	256	331	469	359
D. erecta	49	260	221	113	190	624	220
D. yakuba	49	352	317	49	115	748	145
D. eugracilis	49	555	290	16	54	889	82
D. biarmipes	49	353	392	44	105	819	135
D. triauraria	49	722	265	15	36	1032	66
D. ananassae	49	302	307	80	162	717	190
D. bipectinata	49	769	234	3	33	1033	60
D. persimilis	1.96	292	80	24	10	446	60
D. miranada	2.76	60	120	29	54	259	104
D. willistoni	62.1	1072	135	10	66	1242	91
D. mojavensis	72.63	941	95	21	50	1085	78
D. virilis	72.63	723	217	43	77	1010	104

The genome assemblies are obtained from (Miller et al. 2018; Mahajan et al. 2018).

Supplementary Table S19: Euchromatic regions defined in this study for *D. melanogaster* (BDGP Release 6).

Chromosome	Coordinates
2L	1..22200000
2R	5000000..25479258
3L	1..23400000
3R	4000000..31815305
X	1..21900000

Supplemental Table S20: Structural genomic variants in the polymorphic and divergence datasets used for testing the mode of selection operating upon them at TAD boundaries using Fudenberg and Pollard's method (Fudenberg and Pollard 2019) (Supplemental to Figure 6F).

SV Types	Num.	Cov. (Mb)	Exp. breaks	Exp. Cov. (kb)	Obv. breaks	Exp. Cov. (kb)	Breakpoints: Log10(O/E)	Coverage: Log10(O/E)
Dmel								
Total INS	83,083	6.06	6,121	446.13	3,914	364.00	-0.19	-0.09
1-10 bp INS	49,912	0.22	3,677	16.00	2,450	10.10	-0.18	-0.20
11bp - 20kb INS	33,171	5.84	2,444	430.13	1,464	353.90	-0.22	-0.08
Toal DEL	158,075	1.93	23,290	142.38	19,044	94.034	-0.09	-0.18
1-10 bp DEL	123,395	0.41	18181	30.08	15,135	23.51	-0.08	-0.11
11bp - 2kb DEL	34,680	1.52	5109	112.30	3,909	70.53	-0.12	-0.20
Toal TE	7,132	32.75	525	2,412.43	405	1,514.60	-0.11	-0.20
LTR	3,536	23.80	260	1753.00	154	1005,38	-0.23	-0.24
LINE	2,242	6.95	165	511.73	124	333.25	-0.12	-0.19
DNA-type	1,352	2.00	100	147.61	127	175.98	0.11	0.08
DUP (TD)	1,803	3.16	266	232.80	181	152.43	-0.17	-0.18
Dsim								
Total INS	285,409	4.76	21,026	350.82	18,269	372.90	-0.06	0.03
1-10 bp INS	184,329	0.76	13,579	56.24	11,287	48.09	-0.08	-0.07
11bp - 20kb INS	101,080	4.00	7446	194.58	6,982	324.81	-0.03	0.04
Toal DEL	510,798	4.14	75,259	305.17	68,093	272.629	-0.04	-0.05
1-10 bp DEL	398,117	1.40	58,657	102.95	54,599	0.92	-0.03	-0.05
11bp - 2kb DEL	112,681	2.74	16,602	202.22	13,494	181.70	-0.09	-0.05
Toal TE	1,816	3.73	134	274.71	120	254.72	-0.05	-0.03
LTR	396	2.07	29	152.61	28	130.47	-0.02	-0.07
LINE	527	1.06	39	77.70	34	62.00	-0.06	-0.10
DNA-type	902	0.60	66	44.45	60	62.49	-0.04	0.15
DUP (TD)	1,291	1.40	190	103.38	287	177.56	0.18	0.23
Dmira								
DUP (TD)	1,364	2.38	181	157.84	293	363.66	0.21	0.36

Note: We assigned two breakpoints for each deletion (DELs) or tandem duplication (DUP), and one breakpoint for each insertion (INS) or TE insertion.

Supplemental Table 21: Combinations of parameters tested for each TAD annotation tool.

HiCExplorer	hicFindTADs --correctForMultipleTesting fdr --m hic_corrected.h5 | hic_corrected_5K.h5 | hic_corrected_10K.h5 | hic_corrected_20K.h5 --delta 0.01 | 0.04 --minBoundaryDistance 5000 | 20000 --thresholdComparisons 0.05 | 0.01 | 0.005 | 0.001 **hicFindTADs -m hic_corrected_5K.h5 --correctForMultipleTesting fdr --delta 0.04 --minBoundaryDistance 20000 --thresholdComparisons 0.001**
Juicer Arrowhead	java -Xmx20g -jar /data/apps/juicer/1.5.6/scripts/juicer_tools.jar arrowhead -k NONE --ignore_sparsity inter_30.hic dpse_arrowhead -r 5000 | 10000 **java -Xmx20g -jar /data/apps/juicer/1.5.6/scripts/juicer_tools.jar arrowhead -k NONE -r 5000 --ignore_sparsity inter_30.hic dpse_arrowhead**
Armatus	Armatus -m -S -r 5000 | 10000 | 20000 | 25000 | 40000 | 50000 -s 0.1 | 0.05 -g 1.0 | 2.0 | 0.9 **armatus -S -g 0.9 -r 5000 -s 0.1 -i 5K.matrix -o 5K.out**

The optimal parameters for each tool are highlighted below and used in this study.

Supplemental Figures

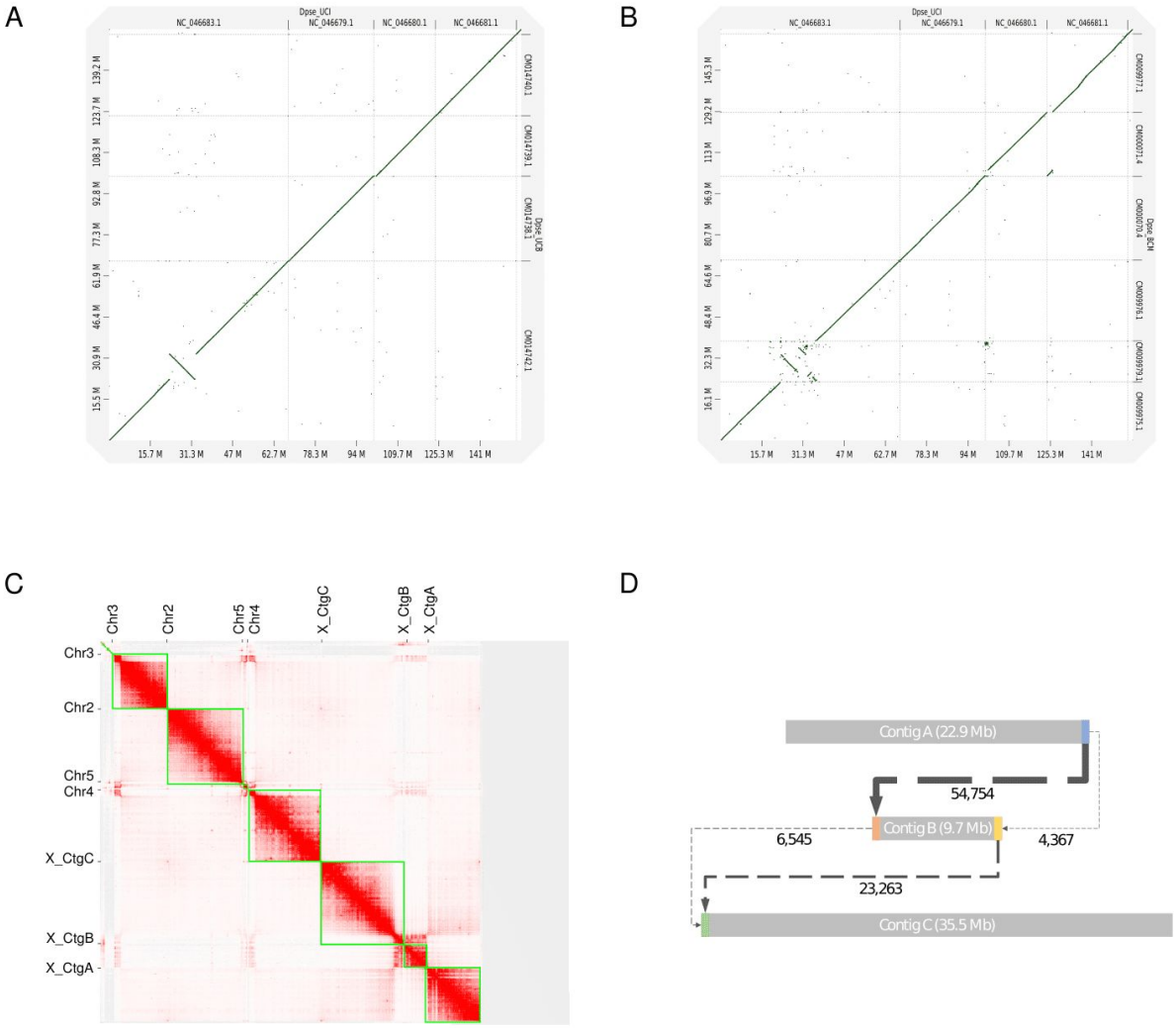

Supplemental Figure S1: A large pericentromeric inversion (9.7Mb) on the X-chromosome of *D. pseudoobscura* between the current assembly and the previous assemblies of this species. (A) Whole-genome alignment plot between the current assembly and the UCB assembly (Mahajan et al. 2018). (B) Whole-genome alignment plot between the current assembly and the FlyBase Dpse_4.0 assembly (English et al. 2012). (C) Hi-C contact map verified the highly continuous contigs and supported the scaffolding of the three contigs of the X-chromosome. (D) Local Hi-C contact frequency data further supported the scaffolding of the three contigs for the X-chromosome.

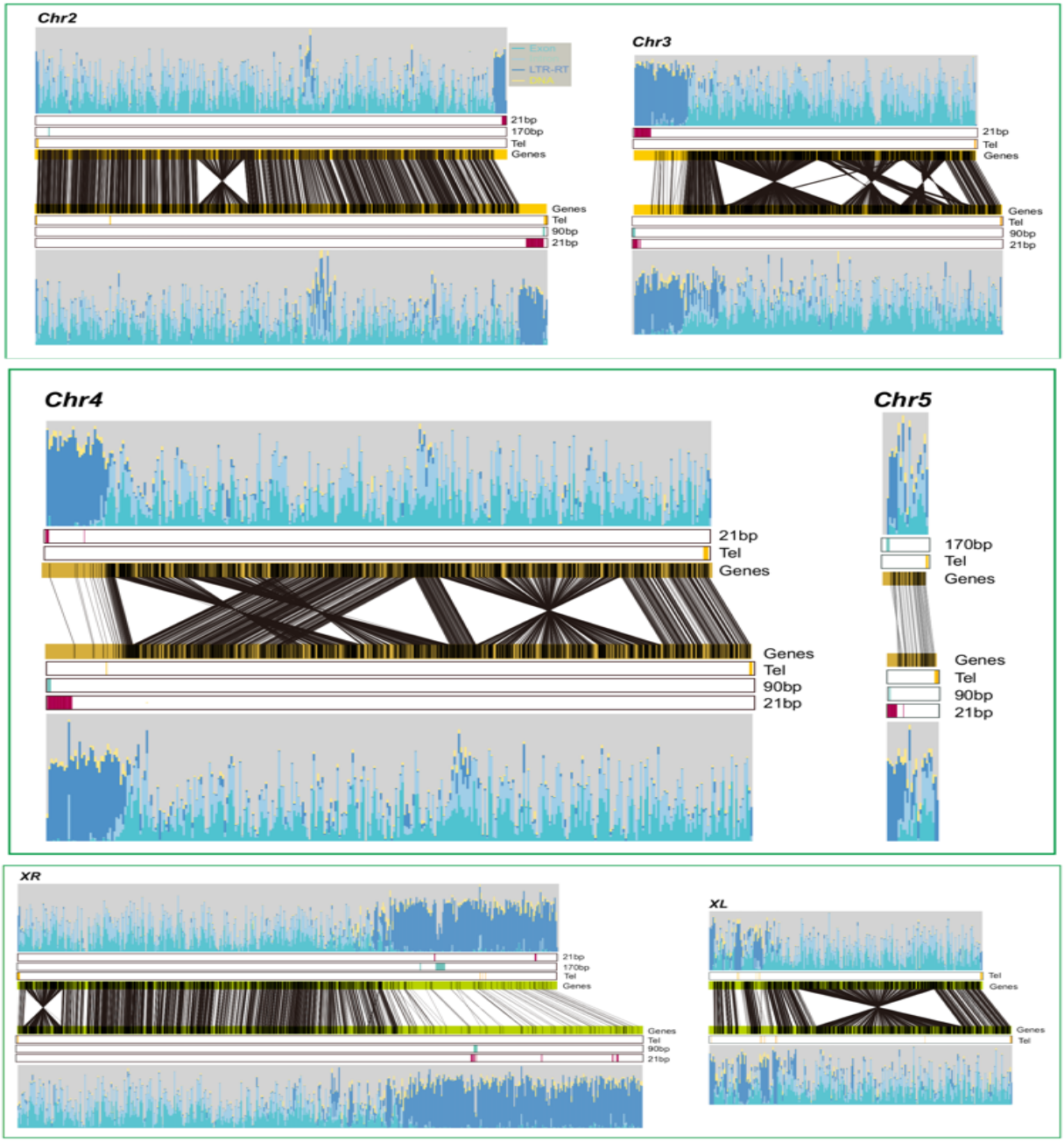

Supplemental Figure S2: Comparative genomic analysis of genome features between *D. pseudoobscura* (this study) and *D. miranda (Mahajan et al. 2018)*. Although their genomes were shuffled by several large rearrangements, the distribution of genomic features (i.e. repeat and gene content) is generally preserved.

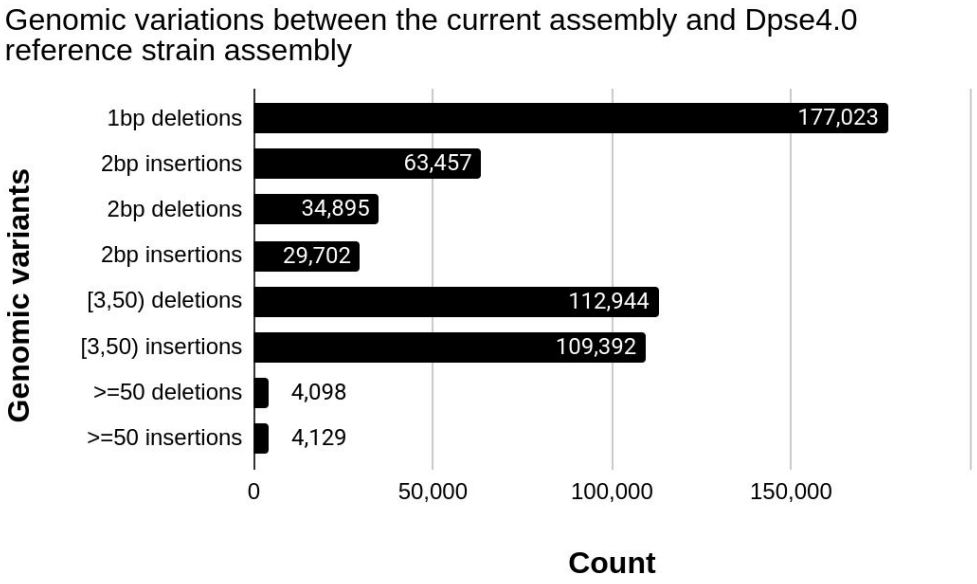

Supplemental Figure S3: Genomic variations identified between the current assembly and the *Dpse4.0* assembly from the reference strain MV2-25. The genomic variants were identified using Paftools (https://github.com/lh3/minimap2/tree/master/misc) within ~140 Mb alignable regions both with single coverage between assemblies. Additionally, there are a total of 1,434,692 SNPs were called between these two assemblies.

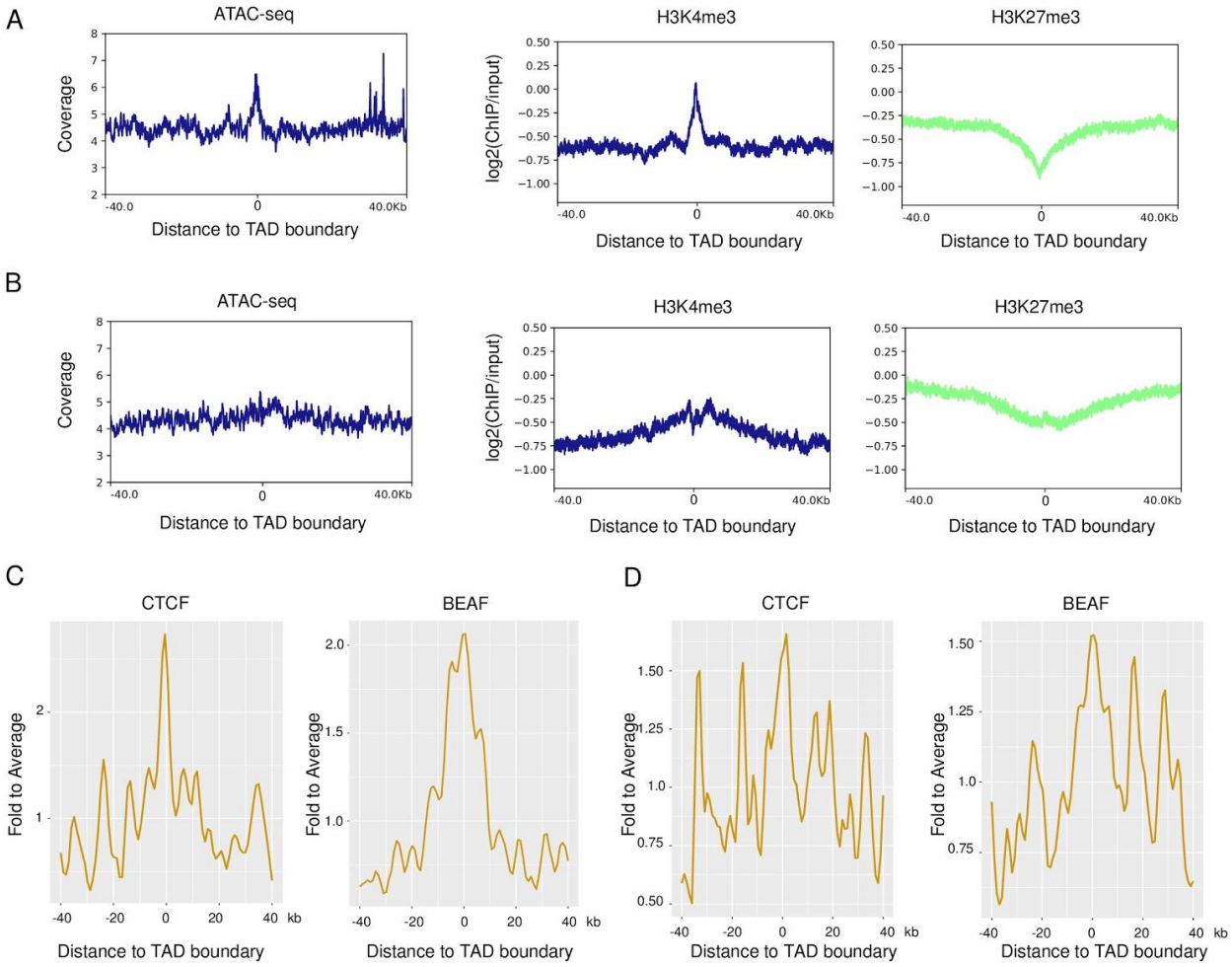

Supplemental Figure S4: Enrichment analysis of insulator binding sites (BEAF-32 and CTCF), epigenetic marks (H3K4me3 and H3K27me3) and ATAC-seq at TAD boundaries. TAD boundaries in (*A*) and (*C*) were identified using Armatus, TAD boundaries in (*B*) and (*D*) were identified using Arrowhead from the Juicer package (Supplemental to Figure 1).

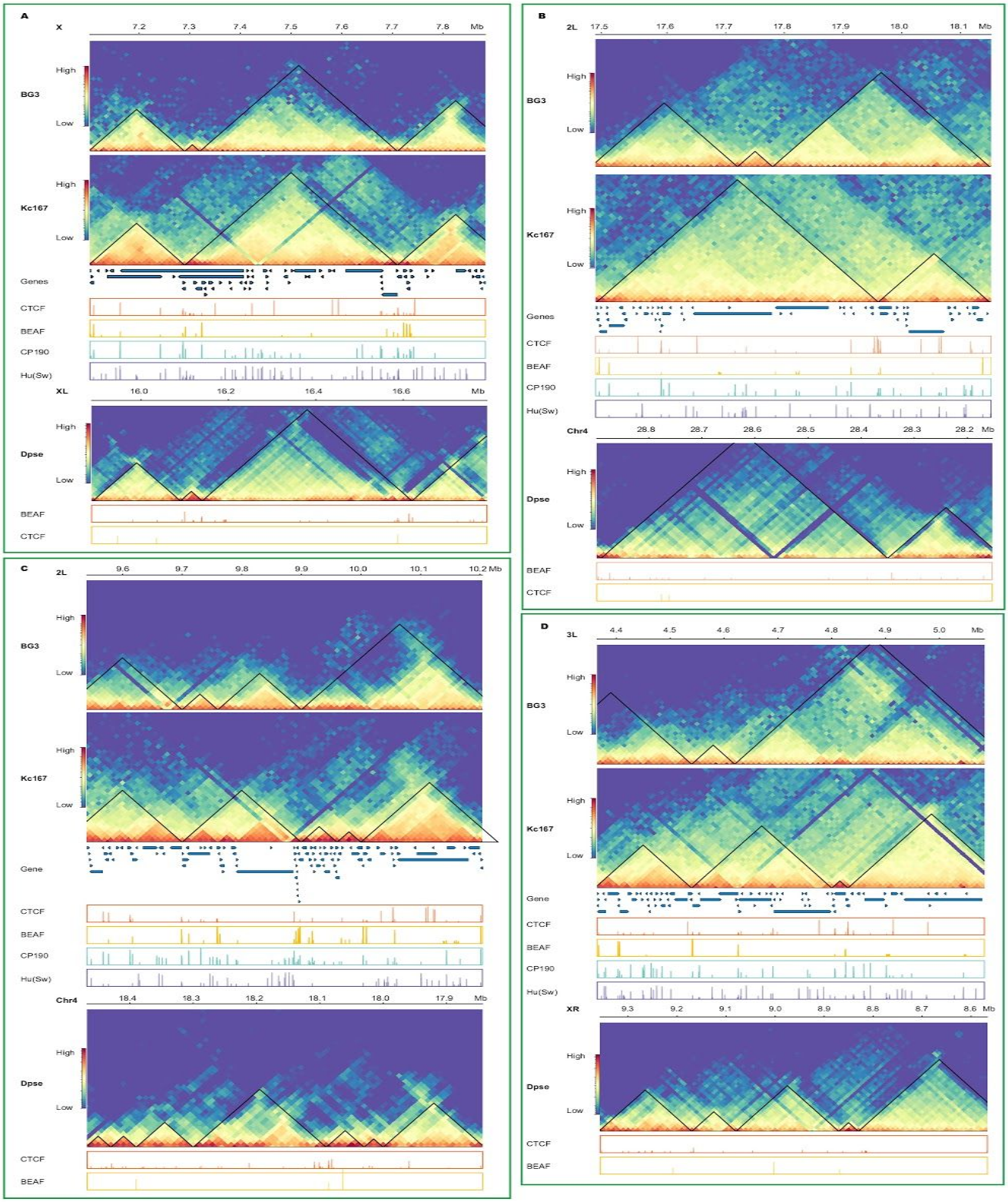

Continued in the next page

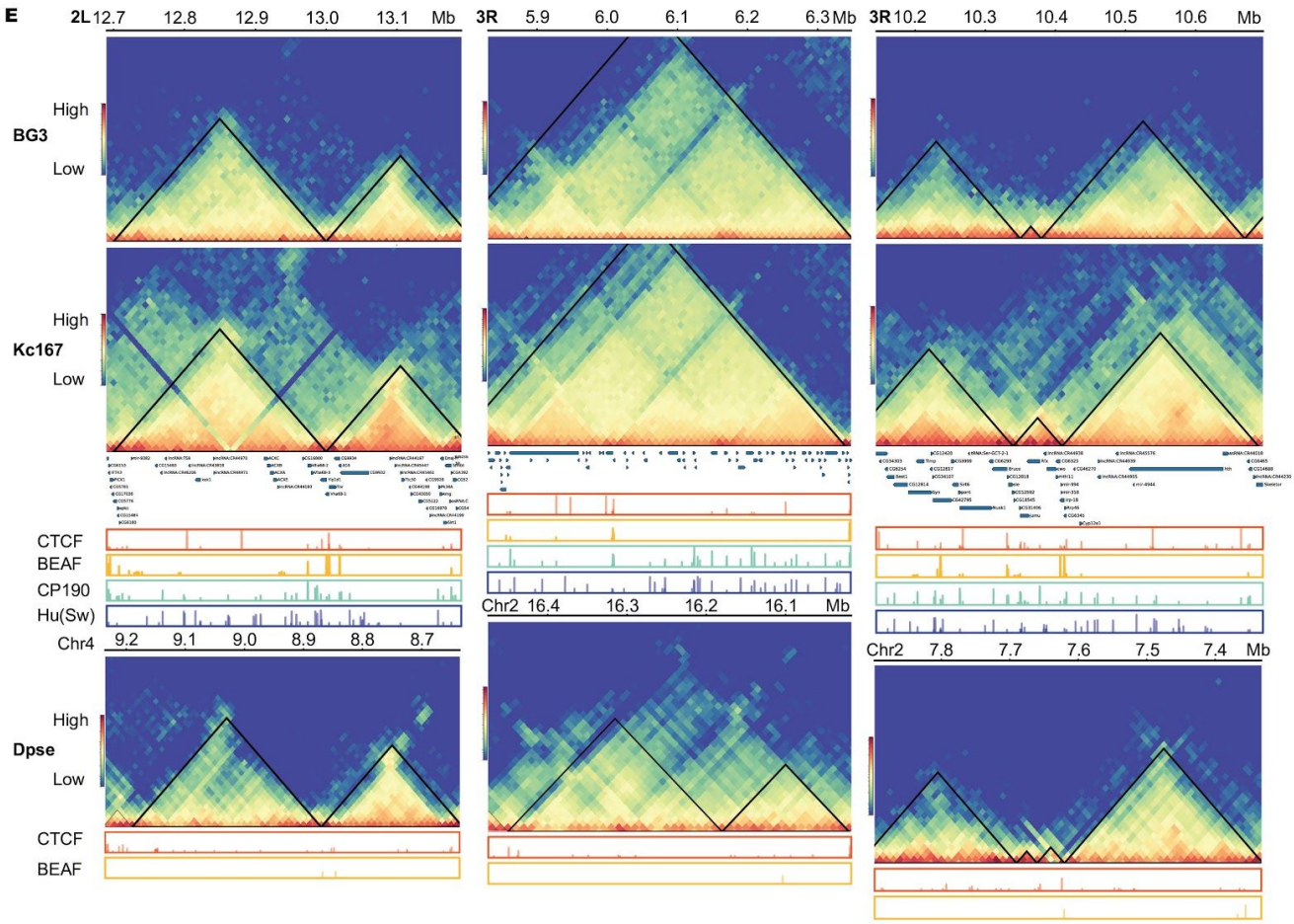

Supplemental Figure S5: Conservation of TADs at the syntenic regions between *D. melanogaster* and *D. pseudoobscura*.

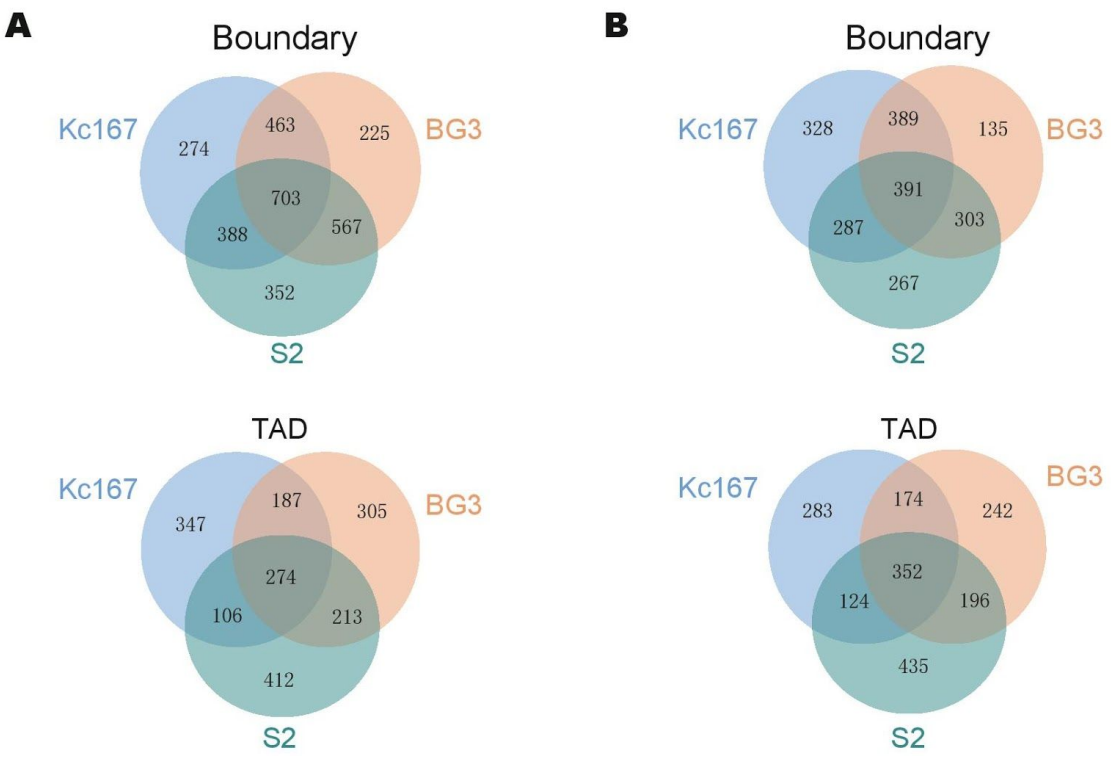

Supplemental Figure S6: TADs are largely shared across cell lines in *D. melanogaster*. (*A*) TADs from three different cell lines (Kc167, BG3, and S2) identified using Armatus. (*B*) TADs identified using Arrowhead.

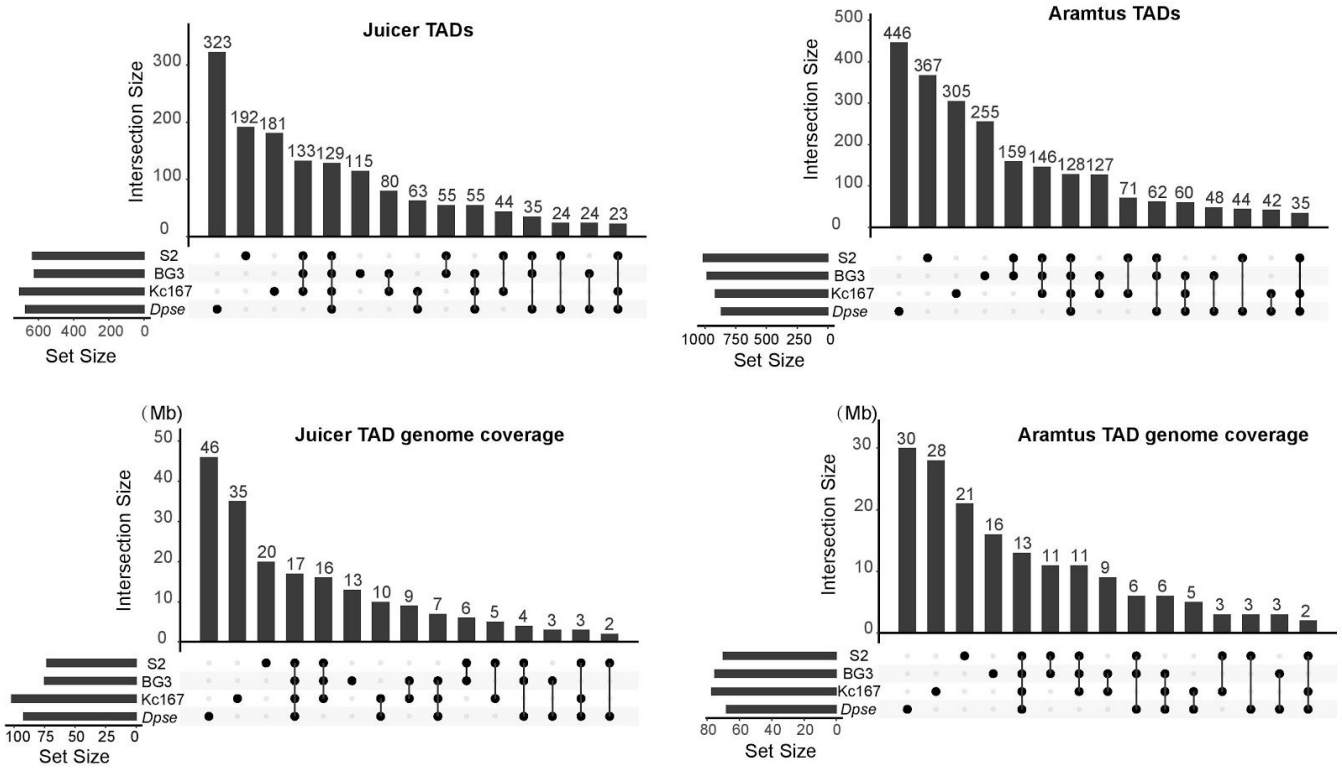

Supplemental Figure S7: Upset plot showing the overlap of TAD structures among three cell lines in *D. melanogaster,* as well as *D. pseudoobscura* whole body (Supplemental to Figure 2). (Left) TADs were identified using Arrowhead from the Juicer package; (Right) TADs were identified using Armatus.

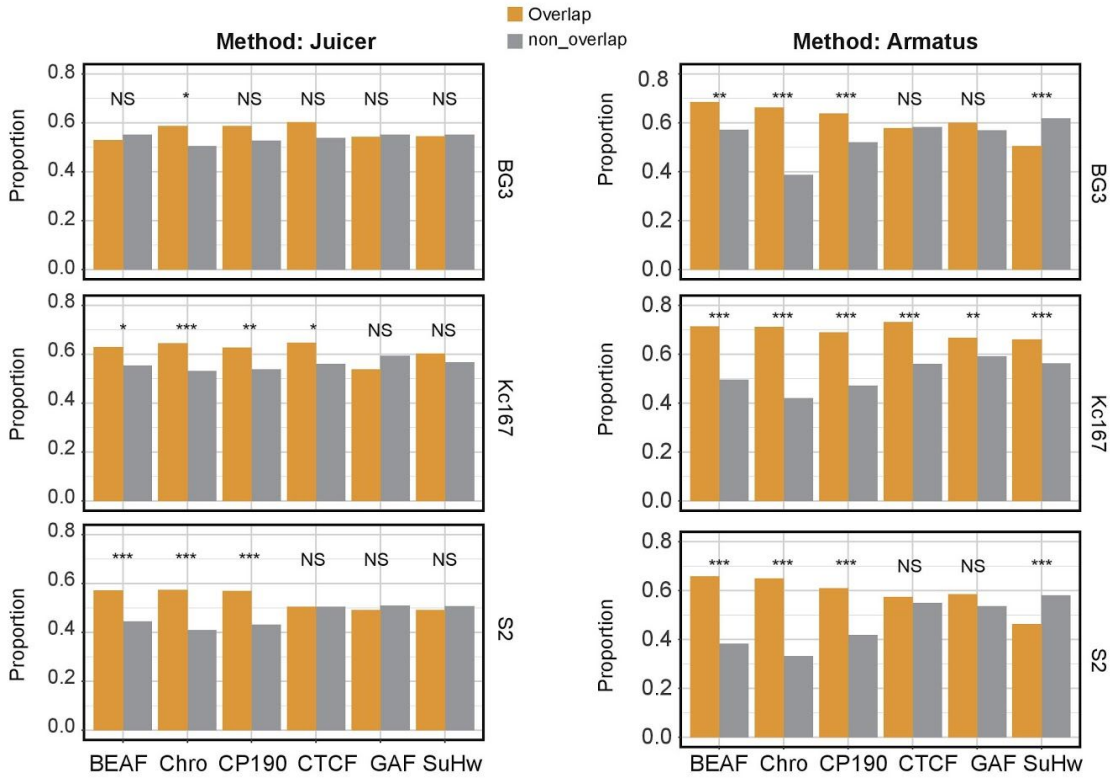

Supplemental Figure S8: Conservation of TAD boundaries that overlapped with different insulator binding sites including BEAF-32, Chro, CP190, CTCF, GAF (Trl) and Su(Hw) between *D. melanogaster* (Kc167, BG3, and S2) and *D. pseudoobscura* (full body) (Supplemental to Figure 3). (Left), TAD boundaries were identified using Arrowhead from the Juicer package; (Right), TAD boundaries were identified using Armatus.

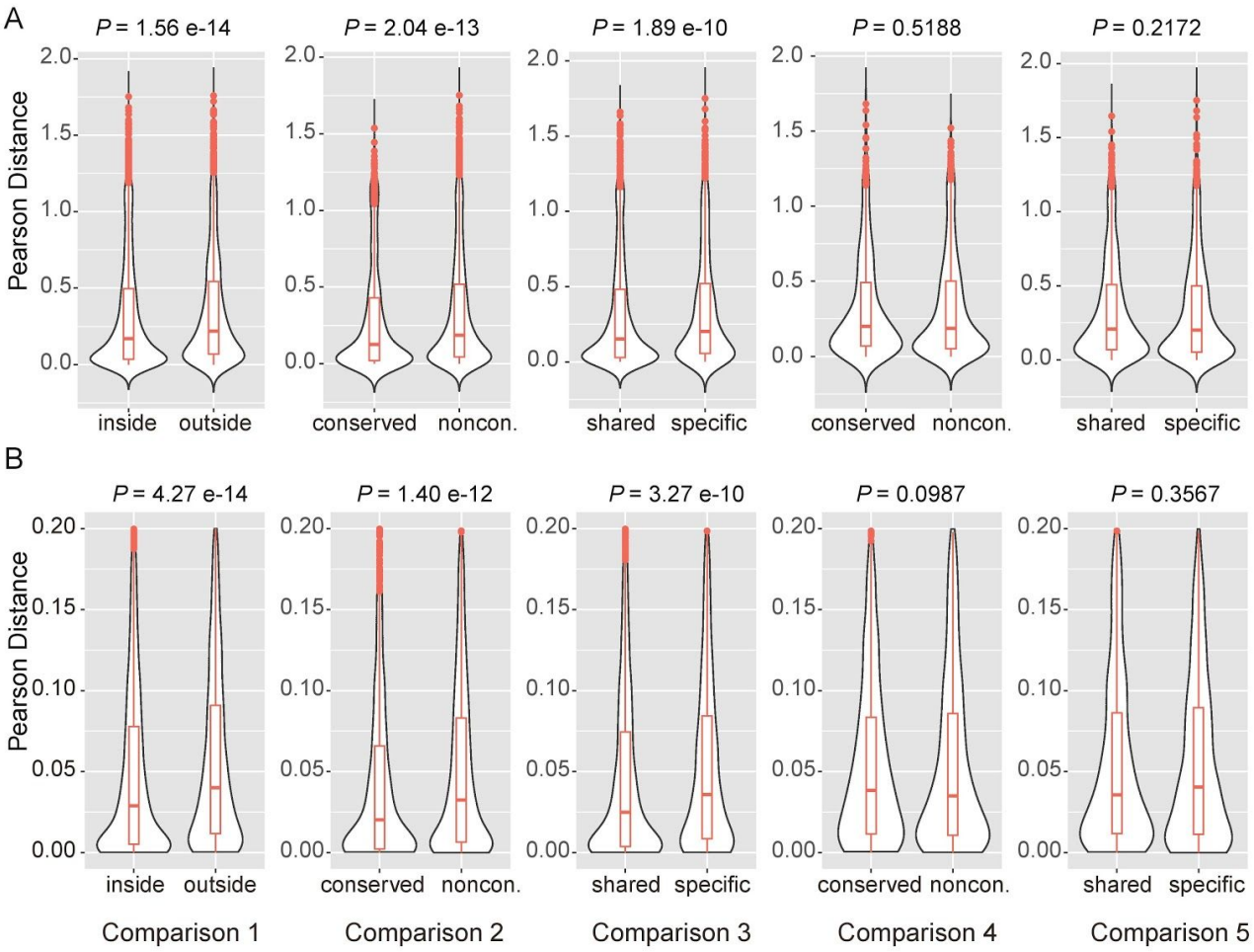

Supplemental Figure S9: The potential roles of TADs in gene regulation in *Drosophila* (Supplemental to Figure 4). (*A*) Expression divergence measured by Pearson's correlation coefficient distance for one-to-one orthologs between *D. melanogaster* and *D. pseudoobscura*. (*B*) Expression variation measured by Pearson's correlation coefficient distance for the same gene sets used in the above interspecific comparison between two *D. melanogaster* strains, OreR and w1118.

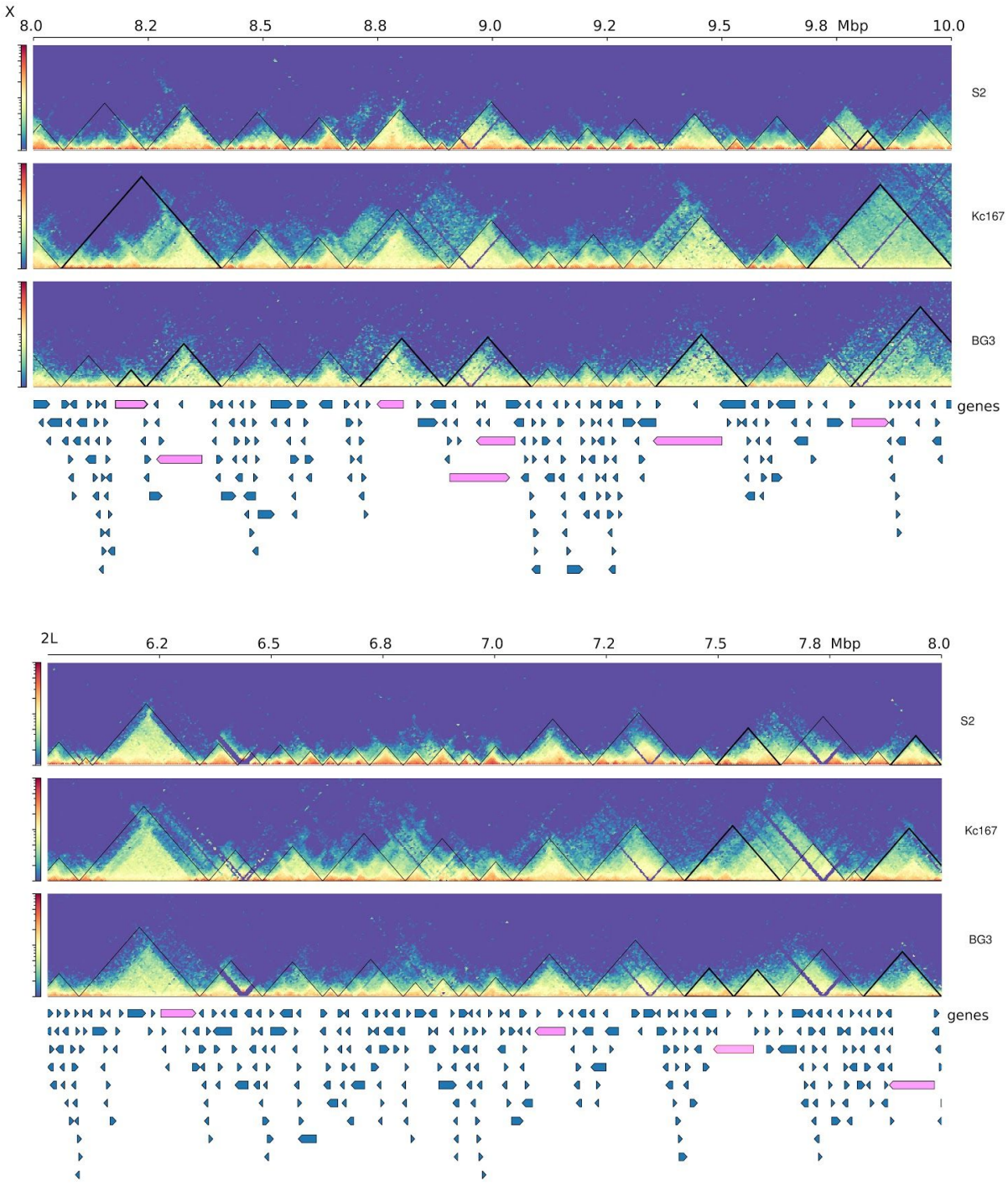

Supplemental Figure S10: Long coding genes (>50 kbp) tend to span full TADs observed in *D. melanogaster*. Top panels represent TADs that were annotated in three *D. melanogaster* cell lines. Below represent gene structures with long genes highlighted in pink color.

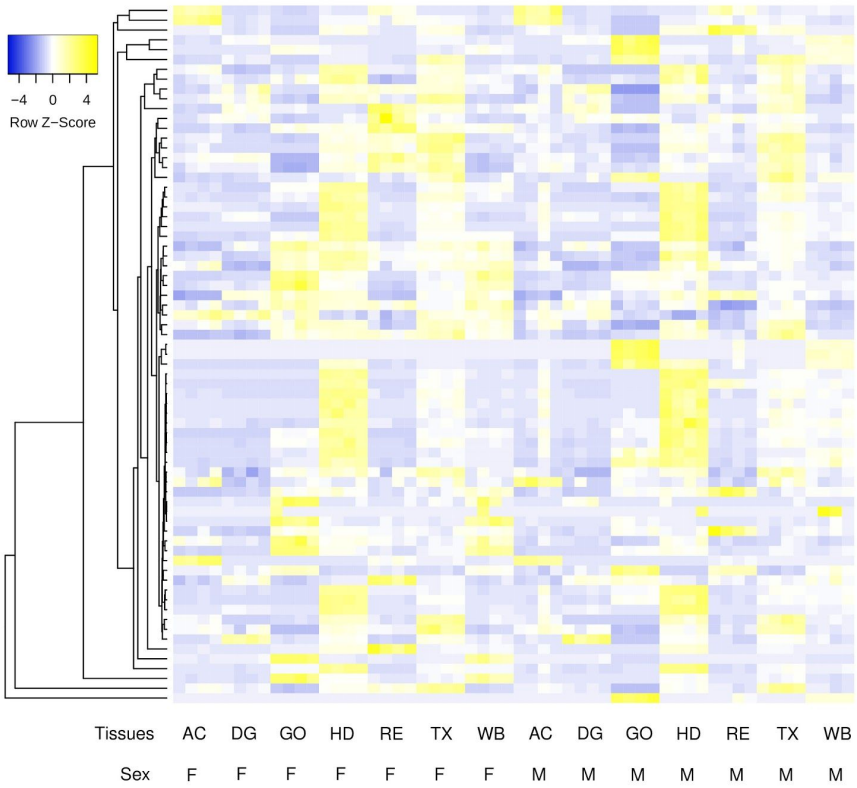

Supplemental Figure S11: Expression profile of 71 long genes (> 50 kbp) that overlapped with complete TADs across 7 tissues from both sex in *D. pseudoobscura* (Supplemental to Figure 4). Long genes are preferentially expressed in the head. AC, abdomen without digestive or reproductive system; DG, digestive plus excretory system; GO, gonad; HD, head; RE, reproductive system without gonad; TX, thorax without digestive system; WB, whole body. F, female; M, male.

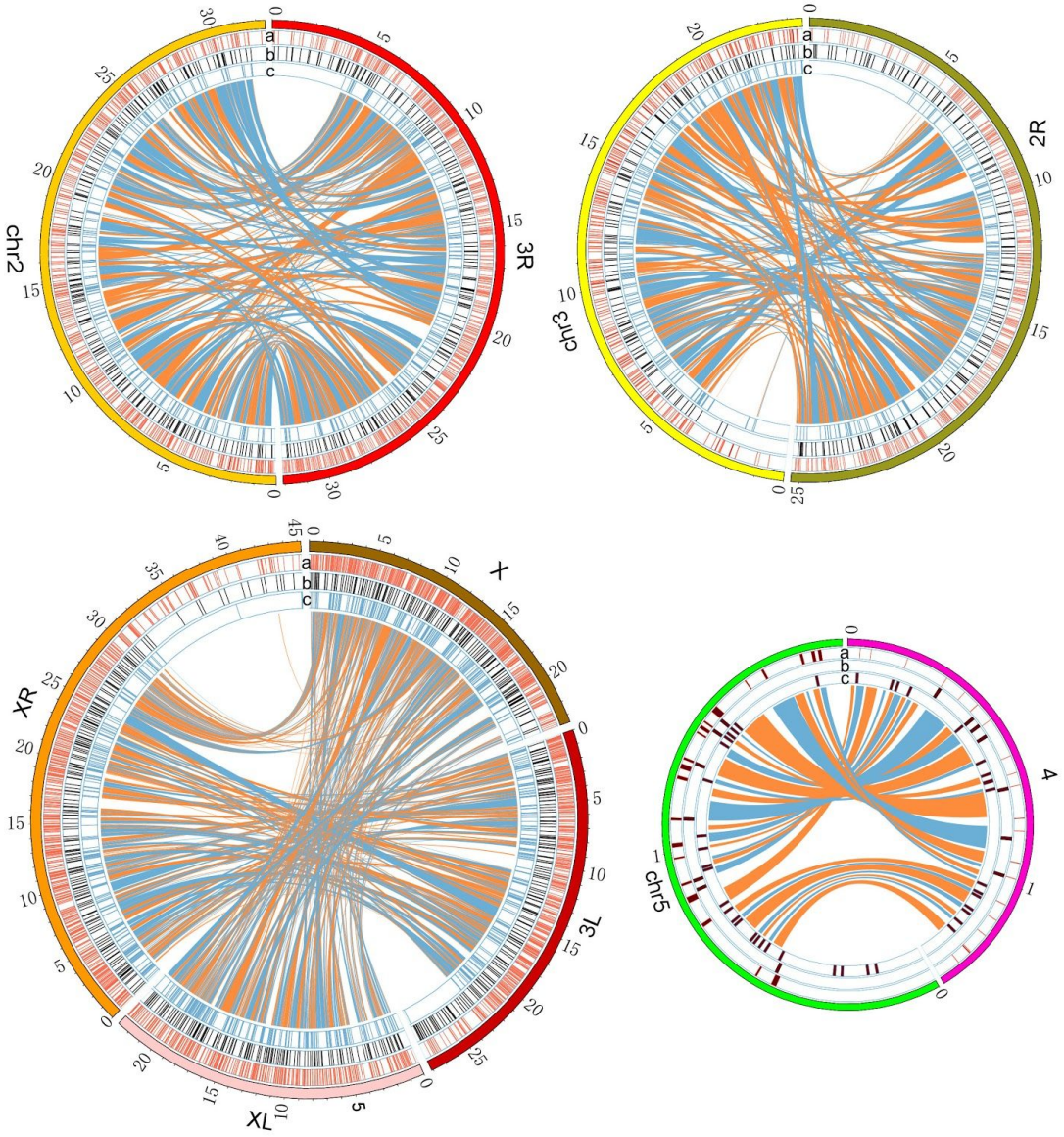

Supplemental Figure S12: Synteny map between *D. melanogaster* and *D. pseudoobscura* (Supplemental to Figure 5A). Tracks a: TAD boundaries annotated by HiCExperor at restriction fragment resolution; b: 10 kbp resolution; c: Synteny breakpoints.

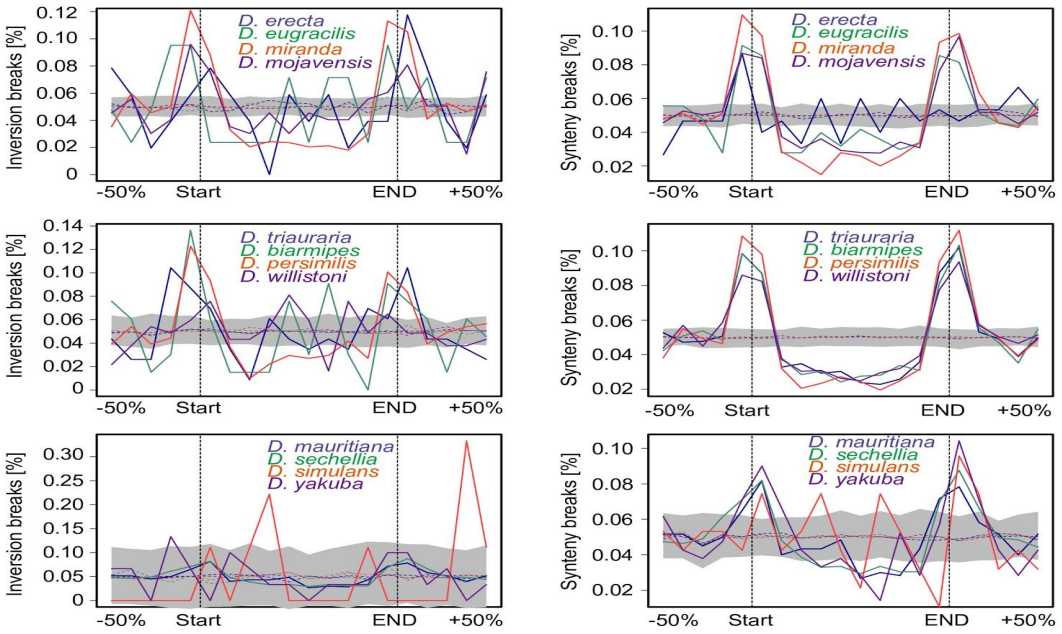

***D. melanogaster* TAD**

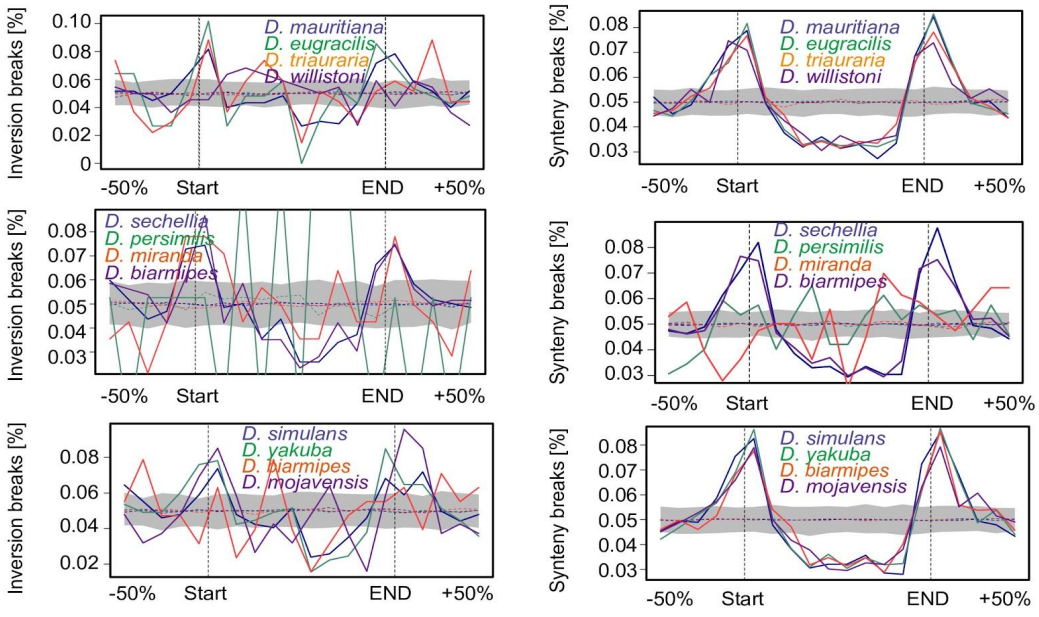

***D. pseudoobscura* TAD**

Supplemental Figure S13: Distribution of evolutionary synteny/inversion breakpoints around TAD boundaries (Supplemental to Figure 5*C*,*D*). (Top) Distribution of genome rearrangement breakpoints between *D. melanogaster* and twelve other *Drosophila* species along TAD regions. (Bottom) Comparisons in *D. pseudoobscura*.

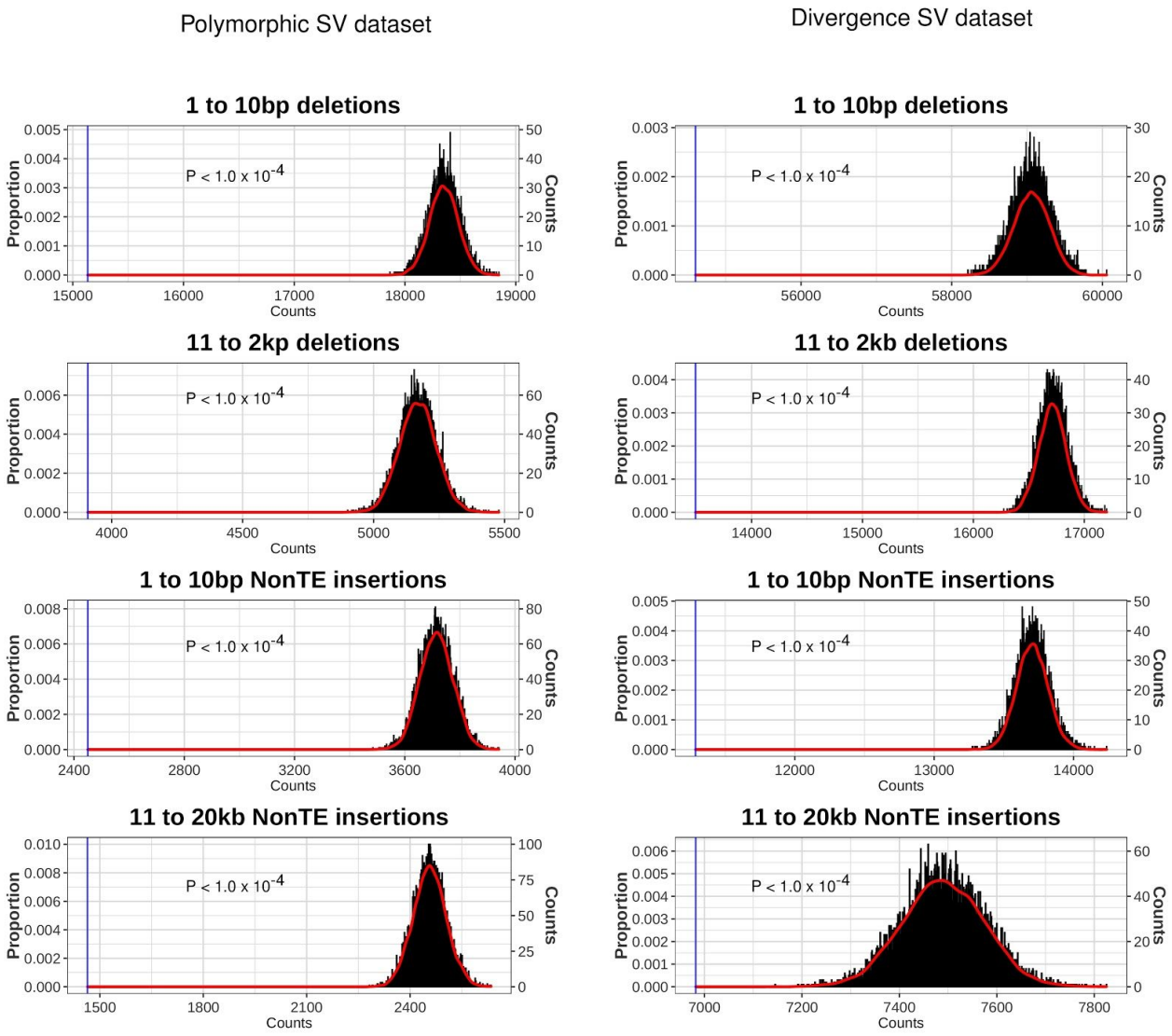

Supplemental Figure S14: Permutation tests (n= 10,000) for evaluating if deletions and non-TE insertions are significantly enriched or depleted at TAD boundaries. Left shows results for polymorphic dataset with genomic variants genotyped in 14 *D. melanogaster* species. Right shows results for divergence dataset with genomic variants genotyped in three *D. simulans* clade species (*D. mauritania*, *D. simulans* and *D. sechellia*). We simulated 10,000 samples of TAD boundaries coordinates with size and chromosomal distribution confined by the actual dataset. *P*-values were calculated based on the observation against the random distribution of frequency that SVs that overlapped TAD boundaries for each type of mutation. The blue lines represent the observed value in our real datasets.

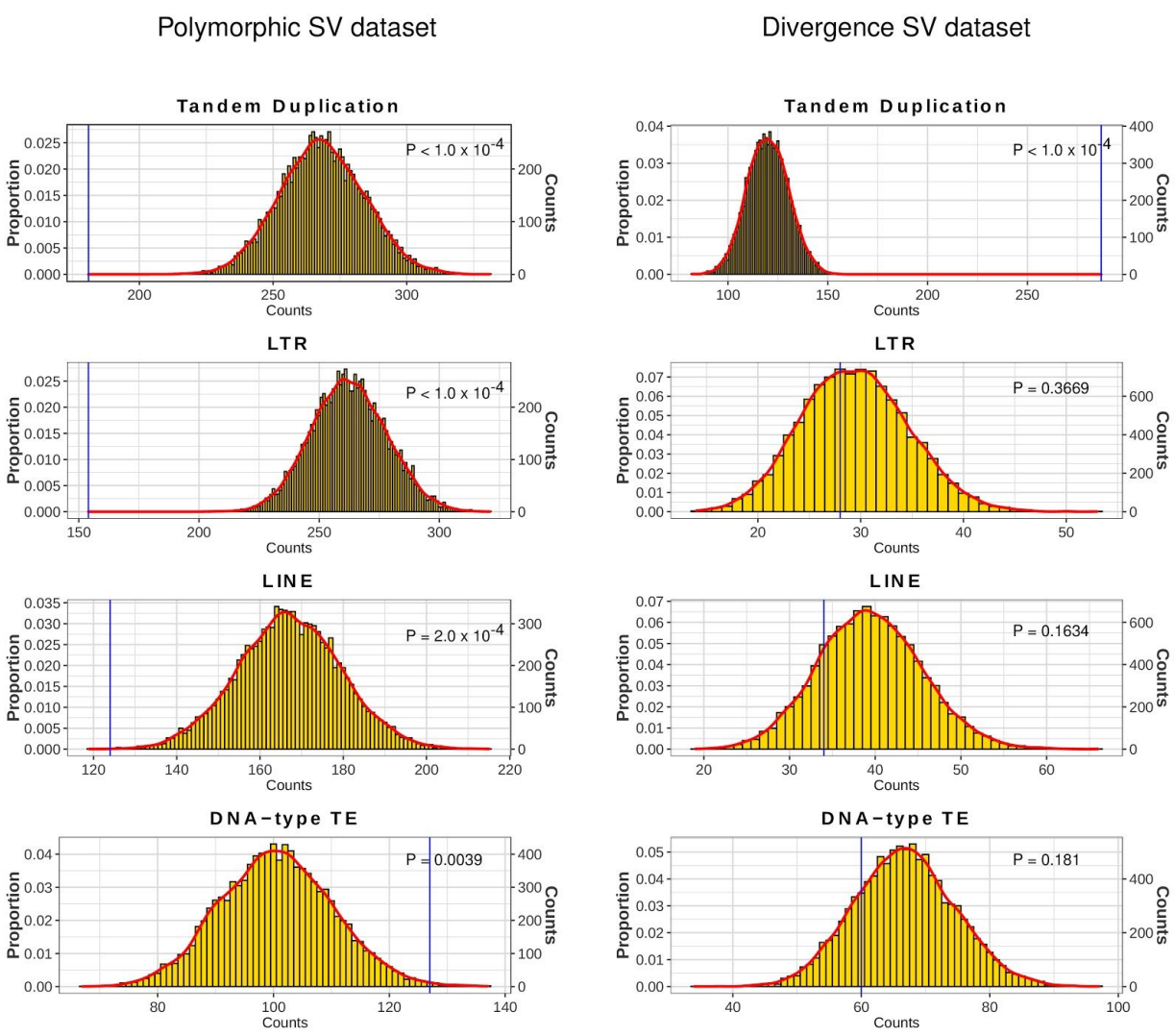

Supplemental Figure S15: Permutation tests (n= 10,000) for evaluating if tandem duplications and three classes of TE insertions (LTRs, LINEs and DNA-type elements) are significantly enriched or depleted at TAD boundaries. Left shows results for polymorphic dataset with genomic variants genotyped in 14 *D. melanogaster* species. Right shows results for divergence dataset with genomic variants genotyped in three *D. simulans* clade species (*D. mauritania*, *D. simulans* and *D. sechellia*). We simulated 10,000 samples of TAD boundaries coordinates with size and chromosomal distribution confined by the actual dataset. *P*-values were calculated based on the observation against the random distribution of frequency that SVs that overlapped TAD boundaries for each type of SVs. The blue lines represent the observed value in our real datasets.

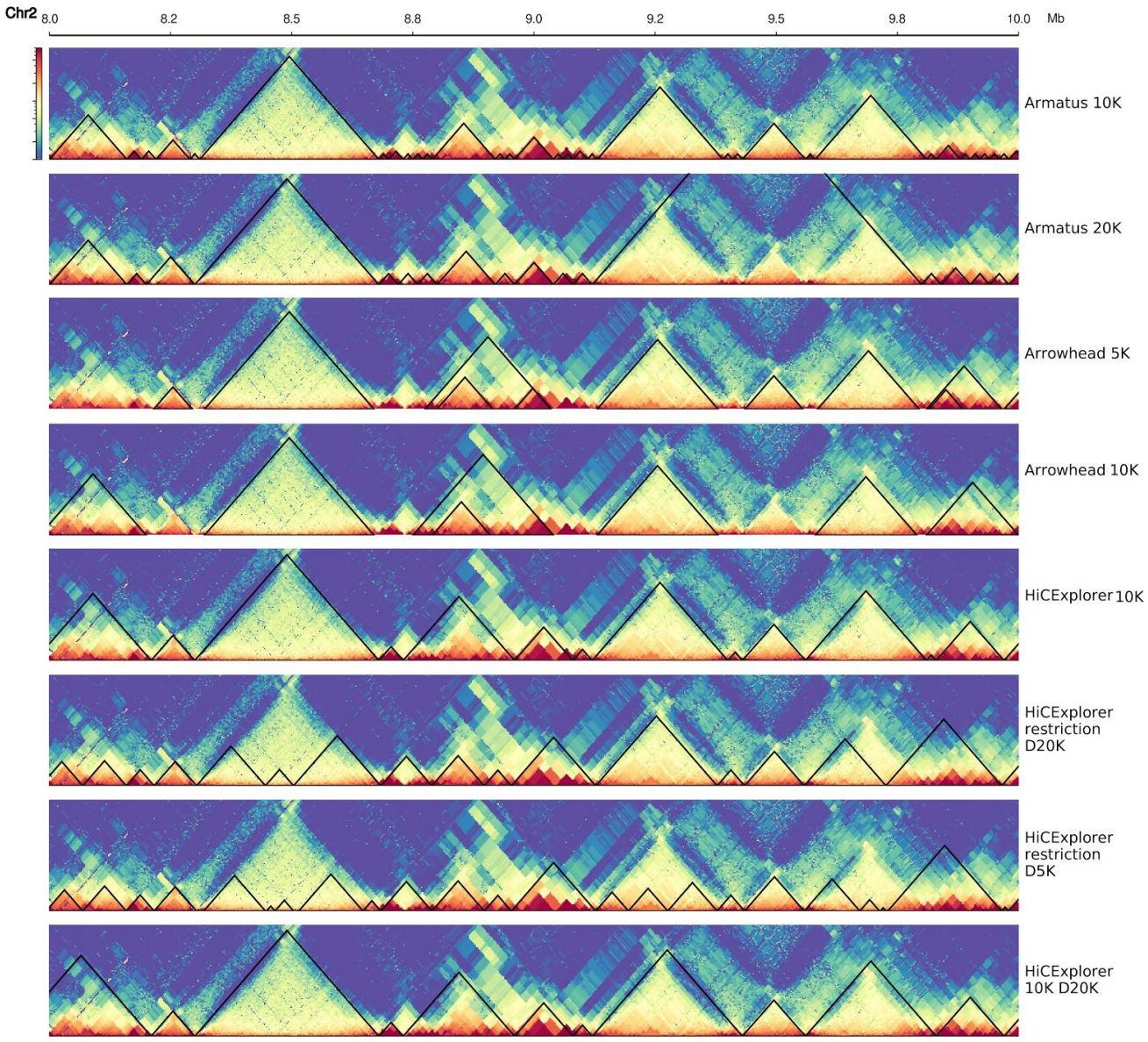

Supplemental Figure S16: Comparison of TAD annotation result for Armatus, Arrowhead in the Juicer package and HiCExplorer under different Hi-C contact map resolutions (restriction fragment resolution, 5 kbp, 10 kbp or 20 kbp). Genomic region on *D. pseudoobscura* chromosome 2 from 8,000,000 to 10, 000,000 (bp) was shown as an example.

Supplemental References

Bracewell R, Chatla K, Nalley MJ, Bachtrog D. 2019. Dynamic turnover of centromeres drives karyotype evolution in Drosophila. *Elife* **8**. http://dx.doi.org/10.7554/eLife.49002.

Campbell MS, Holt C, Moore B, Yandell M. 2014. Genome Annotation and Curation Using MAKER and MAKER-P. *Curr Protoc Bioinformatics* **48**: 188.

Chathoth KT, Zabet NR. 2019. Chromatin architecture reorganization during neuronal cell differentiation in *Drosophila* genome. *Genome Res* **29**: 613–625.

English AC, Richards S, Han Y, Wang M, Vee V, Qu J, Qin X, Muzny DM, Reid JG, Worley KC, et al. 2012. Mind the gap: upgrading genomes with Pacific Biosciences RS long-read sequencing technology. *PLoS One* **7**: e47768.

Fudenberg G, Pollard KS. 2019. Chromatin features constrain structural variation across evolutionary timescales. *Proc Natl Acad Sci U S A* **116**: 2175–2180.

Han Y, Wessler SR. 2010. MITE-Hunter: a program for discovering miniature inverted-repeat transposable elements from genomic sequences. *Nucleic Acids Res* **38**: e199.

He W, Zhao S, Liu X, Dong S, Lv J, Liu D, Wang J, Meng Z. 2013. ReSeqTools: an integrated toolkit for large-scale next-generation sequencing based resequencing analysis. *Genet Mol Res* **12**: 6275–6283.

Kim D, Langmead B, Salzberg SL. 2015. hisat2. *Nat Methods*. https://ccb.jhu.edu/software/hisat2/data/HISAT2-first_release-Sept_8_2015.pdf.

Koren S, Rhie A, Walenz BP, Dilthey AT, Bickhart DM, Kingan SB, Hiendleder S, Williams JL, Smith TPL, Phillippy AM. 2018. De novo assembly of haplotype-resolved genomes with trio binning. *Nat Biotechnol*. http://dx.doi.org/10.1038/nbt.4277.

Mahajan S, Wei KH-C, Nalley MJ, Gibilisco L, Bachtrog D. 2018. De novo assembly of a young Drosophila Y chromosome using single-molecule sequencing and chromatin conformation capture. *PLoS Biol* **16**: e2006348.

Miller DE, Staber C, Zeitlinger J, Hawley RS. 2018. Highly Contiguous Genome Assemblies of 15 Drosophila Species Generated Using Nanopore Sequencing. *G3* **8**: 3131–3141.

Ni X, Zhang YE, Nègre N, Chen S, Long M, White KP. 2012. Adaptive evolution and the birth of CTCF binding sites in the Drosophila genome. *PLoS Biol* **10**: e1001420.

Nozawa M, Onizuka K, Fujimi M, Ikeo K, Gojobori T. 2016. Accelerated pseudogenization on the neo-X chromosome in Drosophila miranda. *Nat Commun* **7**: 13659.

Ou S, Jiang N. 2018. LTR_retriever: A Highly Accurate and Sensitive Program for Identification of Long Terminal Repeat Retrotransposons. *Plant Physiol* **176**: 1410–1422.

Pertea M, Pertea GM, Antonescu CM, Chang T-C, Mendell JT, Salzberg SL. 2015. StringTie enables improved reconstruction of a transcriptome from RNA-seq reads. *Nat Biotechnol* **33**: 290–295.

Riddle NC, Minoda A, Kharchenko PV, Alekseyenko AA, Schwartz YB, Tolstorukov MY, Gorchakov AA,

Jaffe JD, Kennedy C, Linder-Basso D, et al. 2011. Plasticity in patterns of histone modifications and chromosomal proteins in Drosophila heterochromatin. *Genome Res* **21**: 147–163.

Schwartz YB, Linder-Basso D, Kharchenko PV, Tolstorukov MY, Kim M, Li H-B, Gorchakov AA, Minoda A, Shanower G, Alekseyenko AA, et al. 2012. Nature and function of insulator protein binding sites in the Drosophila genome. *Genome Res* **22**: 2188–2198.

Smit AFA, Hubley R, Green P. 2015. RepeatModeler Open-1.0. 2008--2015. *Seattle, USA: Institute for Systems Biology Available from: httpwww repeatmasker org, Last Accessed May* **1**: 2018.

Wang Q, Sun Q, Czajkowsky DM, Shao Z. 2018. Sub-kb Hi-C in D. melanogaster reveals conserved characteristics of TADs between insect and mammalian cells. *Nat Commun* **9**: 188.

Waterhouse RM, Seppey M, Simão FA, Manni M, Ioannidis P, Klioutchnikov G, Kriventseva EV, Zdobnov EM. 2017. BUSCO applications from quality assessments to gene prediction and phylogenomics. *Mol Biol Evol*. http://dx.doi.org/10.1093/molbev/msx319.

Wood AM, Van Bortle K, Ramos E, Takenaka N, Rohrbaugh M, Jones BC, Jones KC, Corces VG. 2011. Regulation of chromatin organization and inducible gene expression by a Drosophila insulator. *Mol Cell* **44**: 29–38.

Xu Z, Wang H. 2007. LTR_FINDER: an efficient tool for the prediction of full-length LTR retrotransposons. *Nucleic Acids Res* **35**: W265–8.

Yang H, Jaime M, Polihronakis M, Kanegawa K, Markow T, Kaneshiro K, Oliver B. 2018. Re-annotation of eight Drosophila genomes. *Life Sci Alliance* **1**: e201800156.

Yang J, Ramos E, Corces VG. 2012. The BEAF-32 insulator coordinates genome organization and function during the evolution of Drosophila species. *Genome Res* **22**: 2199–2207.